Politecnico di Torino

University of Aalborg – wave basin

Performance evaluation test of a 1:26 scaled ISWEC device in extreme wave conditions

Infrastructure Access Reports

Status: Final

Version: 1.0

Date: 21/11/2018

MaRINET2

Experimental analysis of mooring loads in extreme wave condition for floating WEC

ABOUT MARINET

The MaRINET2 project is the second iteration of the successful EU funded MaRINET Infrastructures Network, both of which are coordinated and managed by Irish research centre MaREI in University College Cork and avail of the Lir National Ocean Test Facilities.

MaRINET2 is a €10.5 million project which includes **39 organisations** representing some of the top offshore renewable energy testing facilities in Europe and globally. The project depends on strong international ties across Europe and draws on the expertise and participation of **13 countries**. Over 80 experts from these distinguished centres across Europe will be descending on Dublin for the launch and kick-off meeting on the 2nd of February.

The original MaRINET project has been described as a *"model of success that demonstrates what the EU can achieve in terms of collaboration and sharing knowledge transnationally".* Máire Geoghegan-Quinn, European Commissioner for Research, Innovation and Science, November 2013

MARINET2 expands on the success of its predecessor with an even greater number and variety of testing facilities across offshore wind, wave, tidal current, electrical and environmental/cross-cutting sectors. The project not only aims to provide greater access to testing infrastructures across Europe, but also is driven to improve the quality of testing internationally through standardisation of testing and staff exchange programmes.

The MaRINET2 project will run in parallel to the MaREI, UCC coordinated EU marinerg-i project which aims to develop a business plan to put this international network of infrastructures on the European Strategy Forum for Research Infrastructures (ESFRI) roadmap.

The project will include at least 5 trans-national access calls where applicants can submit proposals for testing in the online portal. Details of and links to the call submission system are available on the project website www.marinet2.eu

European Commission

This project has received funding from the European Union's Horizon 2020 research and innovation programme under grant agreement number 731084.

Document Details	
Grant Agreement Number	731084
Project Acronym	MaRINET2
Title	Performance evaluation test of a 1:20 scaled ISWEC device in extreme wave conditions
Distribution	**Public**
Document Reference	MARINET-TA1-ISWEC 2.0 – 1733
User Group Leader, Lead Author	Mauro Bonfanti Politecnico di Torino mauro.bonfanti@polito.it
User Group Members, Contributing Authors	Panagiotis Dafnakis Politecnico di Torino
Infrastructure Accessed	Aalborg - Wave Basin
Infrastructure Manager or Main Contact	Amélie Tetu

Document Approval Record		
	Name	**Date**
Prepared by	Mauro Bonfanti	29/10/2018
Checked by		
Checked by		
Approved by	Amelie Tetu	21/11/2018

Document Changes Record			
Revision Number	**Date**	**Sections Changed**	**Reason for Change**

Table of Contents

1 Introduction & Background

1.1 Introduction

1.1.1 The ISWEC device

ISWEC (Inertial Sea Wave Energy Converter) is an all enclosed floating gyroscopic WEC, especially designed for the Mediterranean Sea ([1]-[6]). In Figure 1-1, the flywheel is supported by the gyroscope frame and its speed is indicated with φ. The gyro frame is connected to the PTO axis. The speed of the PTO is $\dot{\varepsilon}$. All the energy conversion components are inside a sealed hull that is slack-moored at the seabed. The gyroscope dynamics has been validated and tested on hardware in the loop 1:8 scaled model of the gyroscope unit.

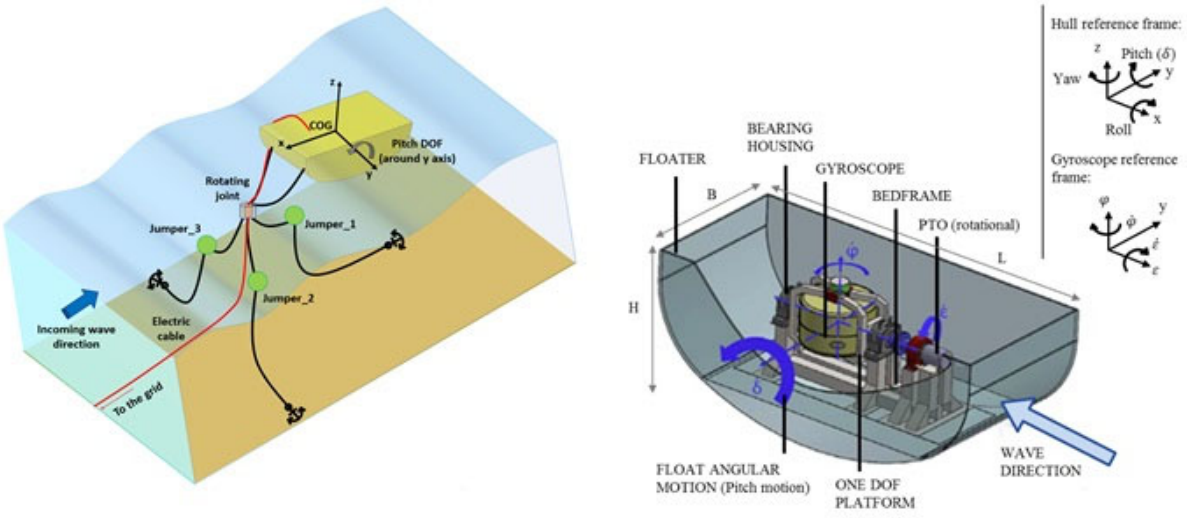

Figure 1-1 The ISWEC device

The Figure 1-1shows a simplified structure of the device carrying inside one gyroscopic unit. The full scale system is composed of a steel-built hull containing two independent gyroscopic units. Each unit is constituted by a flywheel enclosed in a vacuum chamber (yellow part in Figure 1-1) to reduce ventilation losses caused by the air friction. The vacuum chamber is designed to support the flywheel by means of appropriate bearing housings. The gyroscope effect obtained by the combination of the pitch motion and the flywheel rotation induces the vacuum chamber to rotate about the ε axis. This motion drives the PTO. Two radial roller bearings and two spherical roller thrust bearings are used to support both axial and radial loads. Bearings have an oil cooling and lubrication system. The PTO is a mechanical/electrical system composed of a gearbox coupled to an electric generator to increase the low gyroscope speed. An accurate description of the internal components of the full-scale device can be found in ([1]-[6]).

In the first call of MaRINET2, our research group carried out experimental tests at the Hydrodynamic and Ocean Engineering Tank in Nantes (LHEEA). The project concerned the evaluation of the hydrodynamics of different array configurations of ISWEC devices, specifically evaluating the dynamic behaviour of the devices as wave conditions change and consequently the wave field around the bodies. This study was a crucial step in view of the deployment of full-scale array in real sea conditions. Moreover, the coupled dynamic gyroscope/floater has been investigated successfully. The full-scale prototype was deployed and tested offshore Pantelleria Island in the period April 2015-October 2015, to study the behaviour of the device in real sea state conditions. The study performed in this MaRINET call focused on the evaluation of the hydrodynamic behaviour and mooring load in extreme wave conditions in order to design the mooring system of the WEC and compare the results with the numerical model.

1.1.2 Application introduction

The first objective of this experimental campaign is the dynamic study of a floating pitching device in different sea states considering multidirectional waves in order to evaluate the hydrodynamic response of the ISWEC moored device. This study is a crucial step to complete the evaluation on a 1:20 ISWEC device in view of a deployment of

full-scale device and to improve the design method for the mooring system of a pitching WEC. The previous experimental campaign assessed the array hydrodynamic behaviour, without the gyroscopic system. The fundamental objective of this campaign is the comparison of the experimental results in term of body dynamics and mooring load with the numerical results achieved with a time domain model developed in the AQWA environment. The moored device has been studied in regular, irregular and extreme waves considering with different currents. The ability of the device to orient itself in the wave direction has been tested, considering different wave directions and different current intensities. Following this path, it has been possible to have a better understanding of the ISWEC dynamics allowing building a more reliable numerical model for the single device configuration. The experimental results on extreme wave condition has been extremely useful in order to achieve a relevant amount of data in order to carry out a statistical analysis on mooring loads contributing to the progress of mooring design process for wave energy technologies.

1.2 Development So Far

1.2.1 Stage Gate Progress

Previously completed: ✓

Planned for this project: ➲

STAGE GATE CRITERIA	Status
Stage 1 – Concept Validation	
• Linear monochromatic waves to validate or calibrate numerical models of the system (25 – 100 waves)	✓
• Finite monochromatic waves to include higher order effects (25 –100 waves)	✓
• Hull(s) sea worthiness in real seas (scaled duration at 3 hours)	✓
• Restricted degrees of freedom (DofF) if required by the early mathematical models	✓
• Provide the empirical hydrodynamic co-efficient associated with the device (for mathematical modelling tuning)	✓
• Investigate physical process governing device response. May not be well defined theoretically or numerically solvable	✓
• Real seaway productivity (scaled duration at 20-30 minutes)	✓
• Initially 2-D (flume) test programme	✓
• Short crested seas need only be run at this early stage if the devices anticipated performance would be significantly affected by them	✓
• Evidence of the device seaworthiness	✓
• Initial indication of the full system load regimes	✓
Stage 2 – Design Validation	
• Accurately simulated PTO characteristics	✓
• Performance in real seaways (long and short crested)	✓
• Survival loading and extreme motion behaviour.	➲
• Active damping control (may be deferred to Stage 3)	✓
• Device design changes and modifications	✓
• Mooring arrangements and effects on motion	➲
• Data for proposed PTO design and bench testing (Stage 3)	✓
• Engineering Design (Prototype), feasibility and costing	✓
• Site Review for Stage 3 and Stage 4 deployments	✓
• Over topping rates	✓
Stage 3 – Sub-Systems Validation	
• To investigate physical properties not well scaled & validate performance figures	✓
• To employ a realistic/actual PTO and generating system & develop control strategies	✓

STAGE GATE CRITERIA	Status
• To qualify environmental factors (i.e. the device on the environment and vice versa) e.g. marine growth, corrosion, windage and current drag	
• To validate electrical supply quality and power electronic requirements.	✓
• To quantify survival conditions, mooring behaviour and hull seaworthiness	➲
• Manufacturing, deployment, recovery and O&M (component reliability)	✓
• Project planning and management, including licensing, certification, insurance etc.	✓
Stage 4 – Solo Device Validation	
• Hull seaworthiness and survival strategies	➲
• Mooring and cable connection issues, including failure modes	➲
• PTO performance and reliability	✓
• Component and assembly longevity	
• Electricity supply quality (absorbed/pneumatic power-converted/electrical power)	✓
• Application in local wave climate conditions	✓
• Project management, manufacturing, deployment, recovery, etc	✓
• Service, maintenance and operational experience [O&M]	✓
• Accepted EIA	
Stage 5 – Multi-Device Demonstration	
• Economic Feasibility/Profitability	
• Multiple units performance	✓
• Device array interactions	✓
• Power supply interaction & quality	
• Environmental impact issues	
• Full technical and economic due diligence	
• Compliance of all operations with existing legal requirements	

1.2.2 Plan For This Access

Different sea conditions applied to the ISWEC device were tested in this experimental campaign. Specifically, both regular, irregular and extreme waves were considered, having different direction and intensity. Moreover, currents have been generated. This is to evaluate the hydrodynamic behaviour of the system and its mooring loads to validate the simulation software used to carry out the hydrodynamic behaviour of it, to highlight the performance variation under more realistic operating conditions than ideal one.

The plan for this access was:

- Setup of the system and pre-test of the experimental hardware and software layout including wave gauges calibration for regular and irregular waves.
- Single device tests:
  - Still water test for the free decay analysis both in roll, pitch, heave and surge motion
  - 6 DOF free response with moored device for RAO estimation.
  - 6 DOF free response with moored device under irregular waves;
  - 6 DOF free response with moored device under extreme wave;
  - 6 DOF free response with pressure sensor on the hull surface under regular waves;
  - 6 DOF free response with pressure sensor on the hull surface under irregular multidirectional waves;

2 Outline of Work Carried Out

2.1 Experimental setup

2.1.1 Wave basin setup

The wave basin (Figure 2-1) is 14.6 m x 19.3 m x 1.5 m with an active test area of 13 x 10 m. A deep water pit with size 6.5 m x 2.0 m with up to 6 m extra depth is available. The basin holds up to approximately 400 m3 water (400.000 liters) and accommodates testing on deep and shallow water. The basin is equipped with long-stroke segmented piston wavemaker for accurate short-crested (3-dimensional) random wave generation with active absorption and pumps for currents. The wavemakers are powered by electric motors which allow for less acoustic noise, no oil pollution in the basin and more accurate waves. In addition, the tank is equipped with a bridge crane that crosses it along its transversal length.

The equipment wave and current generation system for basin:

- 30 individually controlled wave paddles (snake type configuration) powered by electric motors (Figure 2-2)
- Accurate generation of 3D waves due to narrow vertically hinged paddles (0.43 m segment width)
- Maximum wave height up to 45 cm (at 3 s period)
- Typical maximum significant wave height in the range of 0.25-0.30 m
- Pumps with a total maximum flow of 3500 m3/h for generation of strong current in the basin (up to 0.15 m/s at 0.5 m water depth). Structures can be tested in combined waves and current (following or opposing)
- Passive wave absorber elements (Figure 2-3)

Figure 2-1: Aalborg Wave Basin

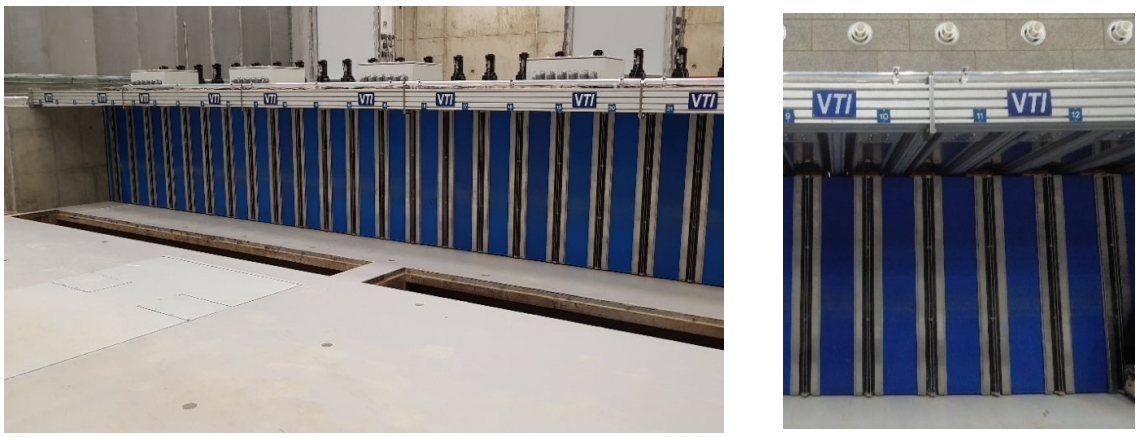

Figure 2-2: Wave maker of Aalborg Wave Basin

Figure 2-3: Passive absorber elements

The facility provided a large number of sensors for wave height measurement and current measurement. Specifically, the wave sensors were resistive wave gauges, one of which is shown in Figure 2-4. These sensors consist of a sensitive part, about 70 cm long, which is partially immersed in the water. As the immersion of the sensitive part varies, the resistance of the same varies and therefore the output signal (in volts) varies. At the beginning of each day of testing, the sensors were calibrated to obtain the calibration curve.

For what concern the current sensor, it was a Vectrino high-resolution acoustic velocimeter used to measure 3D water velocity fluctuations within a very small sampling volume and at sample rates of up to 200 Hz. It can be applied in a variety of environments, from hydraulic labs – where it is regarded as standard equipment – to the ocean. It is ideal for near-boundary flow measurements or to capture any highly dynamic phenomena in a hydraulic tank. Figure 2-4 shows the current sensor: the sensor is equipped with four beams for measuring the flow in all directions of space, making it a multidirectional sensor.

Both the current sensor and the wave gauges have been positioned according to a precise pattern in order to guarantee:

- the measurement of the current at the depth corresponding to half of the draft of the device;
- the acquisition of the wave field around the device (8 wave gauges)
- the acquisition of the undisturbed wave field, considering two wave sensors in order to have a double check on the undisturbed wave field.

Figure 2-4: Resistive wave gauge, current sensor and installation structure

To position the sensors, a tubular structure was attached to the bridge, as shown in Figure 2-4 and Figure 2-5. The positioning scheme is shown in Figure 2-18: as you can see, the positioning of the wave gauges from number 1 to number 8 has been designed to measure the wave field around the device, highlighting the disturbance caused by the motion of the device with respect to the undisturbed field. The latter was measured by the wave probes 9 and 10, as they were positioned laterally and at a distance such as to be considered undisturbed.

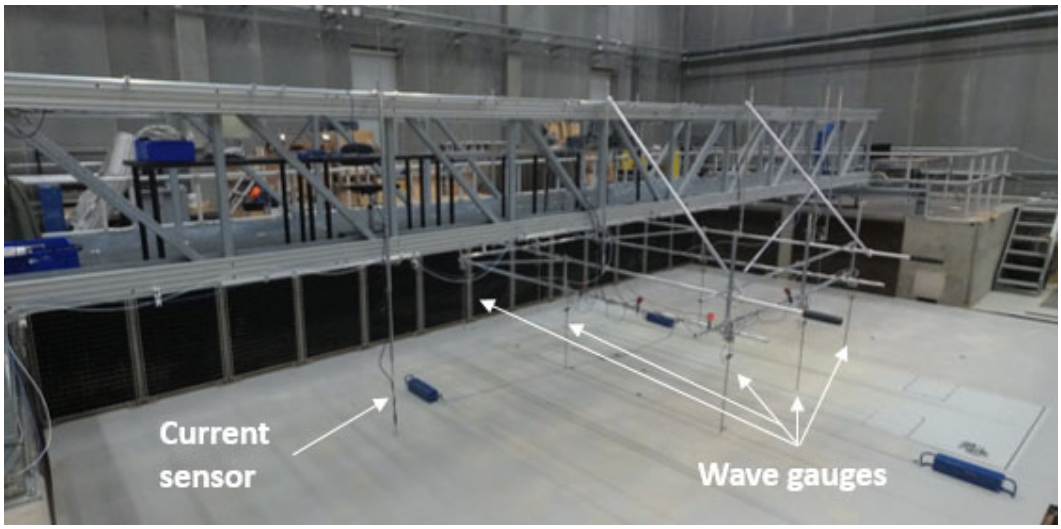

Figure 2-5: Installation structure and support of current sensor and wave gauges

2.1.2 ISWEC device setup

In this experimental campaign, a scaled model has been considered. The floater is a 1:26 scaled prototype of the ISWEC device designed for the Europe north sea. The Froude scaling law have been considered for the scaling of the model geometrical and inertial properties (Table 2-1). In Figure 2-6 and Figure 2-7 the CAD and drawings of the tested model are shown. The draft of the device was checked in the water tank, and the static stability as well was checked with a bubble liver. Once the geometrical and mass properties of the scaled device had been determined and verified, the electrical connections were made and the hull was properly closed with a plexiglass panel to prevent the entry of water (Figure 2-8).

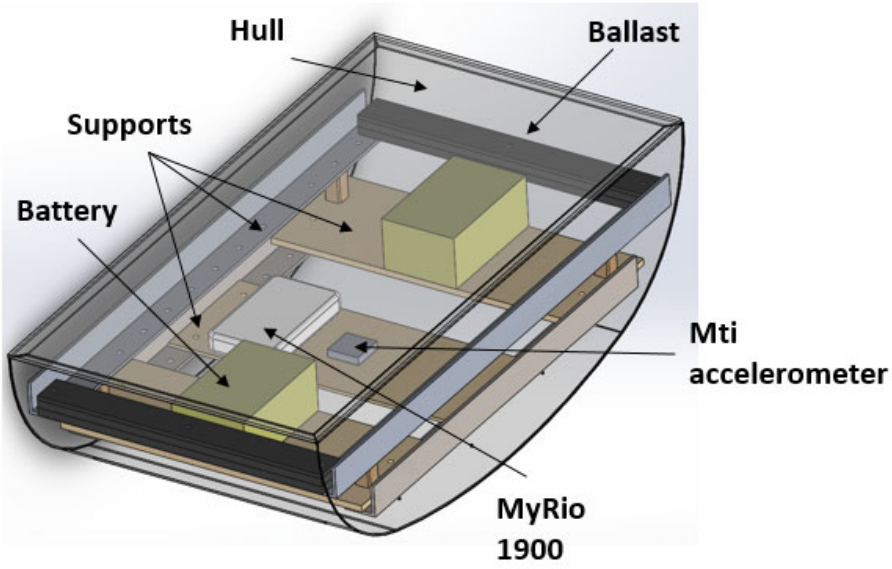

Figure 2-6: CAD of the tested model

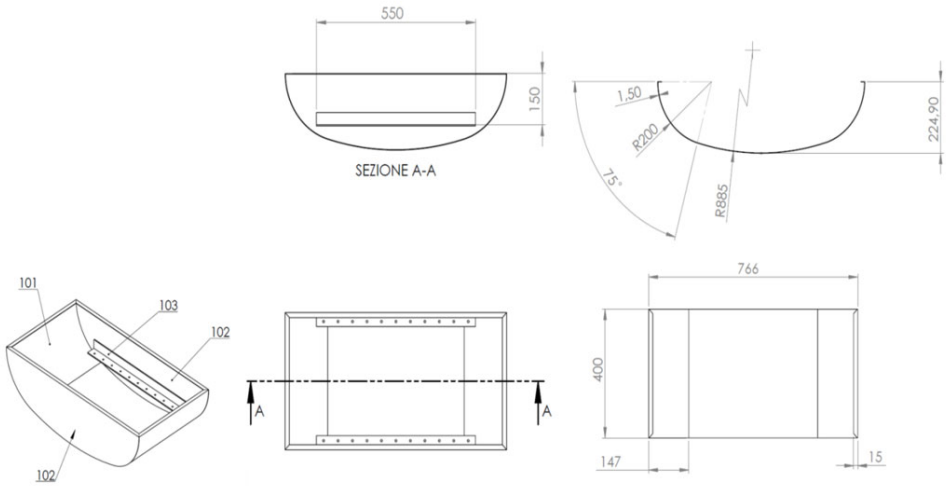

Figure 2-7: Drawing sketches of the hull

	Scaling factor	1:26 scaled device	Full scale device
Length (m)	1	0.75	20
Width (m)	1	0.4	10
Height (m)	1	0.225	5.87
Draft (m)	1	0.15	3.9
Radius 1 (m)	1	0.2	5.2
Radius 2 (m)	1	0.885	23
Total mass (kg)	3	36.443	600000
Roll inertia (kgm^2)	5	0.54	6414219
Pitch inertia (kgm^2)	5	2.41	28420685
Yaw inertia (kgm^2)	5	2.74	32474464
COG from water plane (m)	1	-0.0243462	-0.633
Equivalent J (kgm^2)	5	0.0175	28977
Water depth (m)	1	0.96	25

Table 2-1: Full scale and prototype main features

On board, a Data AcQuisition system (DAQ) is needed to record experimental signals of the physical quantities of interest (Figure 2-8). To perform an analysis of the dynamics of the hull, the motion of the six DoFs of the hull need to be acquired. The floater is equipped with an Inertial Unit of Measurement (IMU) installed on board, at the CoG, to record the device motions. More in details, a Xsens MTi-30 AHRS sensor was used. The sensor was fixed inside the hull on a wood plate in order to be oriented correctly with respect to the hull reference frame. The data acquisition is managed by a National Instrument myRio 1900 which is a Xilinx 667 MHz real time control unit. A UART serial embedded interface allows to communicate with the MTi by means of a RS232 to UART converter. The myRio is equipped with two MXP connectors and one MSP connector that provide several analogical and digital inputs and outputs.

Since the MTi returns only the angular position of the system and the acceleration for the three space direction, another system is needed to acquire the absolute position of the device in water. In this regard, an OptiTrack Flex 13 object tracking system has been employed. As shown in Figure 2-9, this optical system uses four cameras placed in a suitable way to follow the motion of the device. In our case, the markers have been positioned above our hull as shown in Figure 2-10: four markers are necessary to define the rigid body, three markers define a plane and one marker, higher than the others, completes the rigid body creating a 3D solid, obtained by connecting all four markers with segments. In this way, the optical system is able to recognize a 3D rigid body and to define its movement. During the acquisition, the system saved the position X, Y, Z of the centre of gravity of the rigid

body defined by the markers, its angular position and the position X, Y, Z of each single marker. The Optitrack system was equipped with 4 "Flex 13" cameras with a capture volume 8 Ø × 7 feet, 2 Ø × 2 meters of setup area, and 6 Ø meters Drones/Robots/Objects.

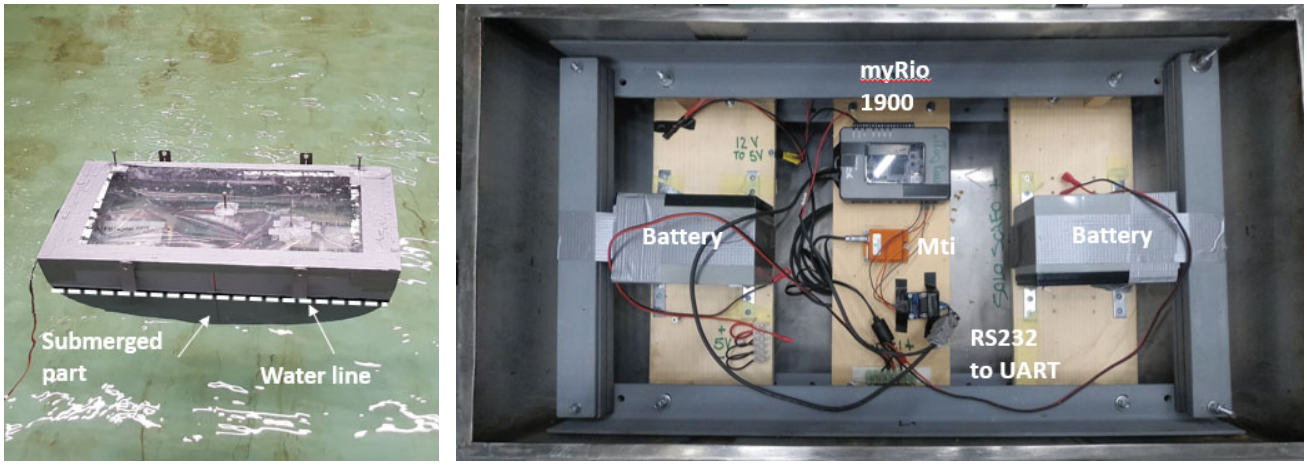

Figure 2-8: ISWEC model ready for the test and its acquisition system

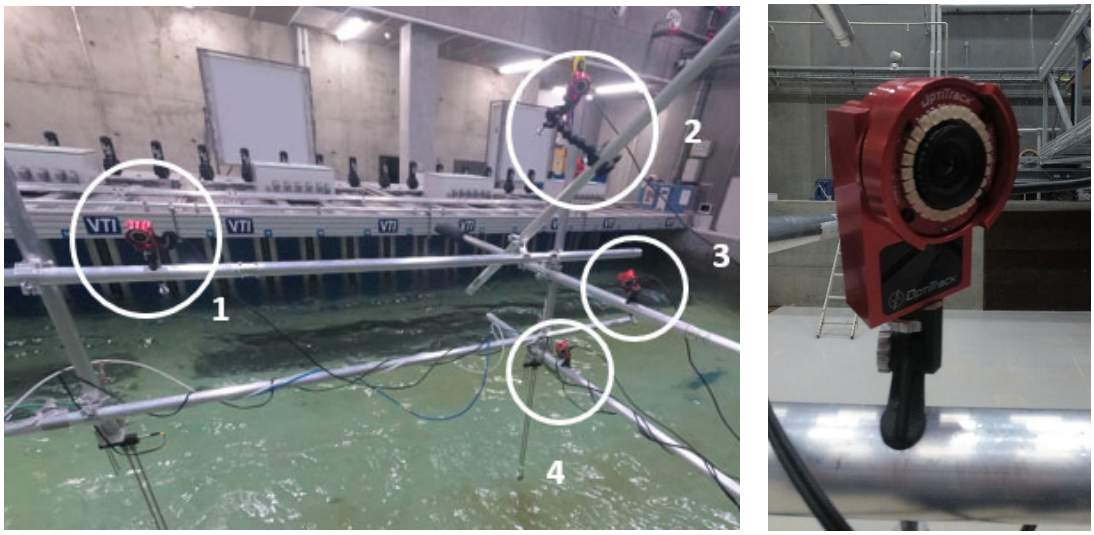

Figure 2-9: Optitrack camera installation

Figure 2-10: ISWEC model with Optitrack markers

Moreover, another hull was equipped with analogue pressure sensors in order to evaluate the pressure field on the hull surface. The "pressure" hull was the same hull used for extreme wave tests. 11 holes on its wetted surface were made in order to install 11 pressure sensors (ABP D AN T 001PG A A 5, Honeywell analogue pressure sensor, 0 to 1 psi, from Mouser). Below is reported a scheme of the setup and acquisition system of the pressure sensors:

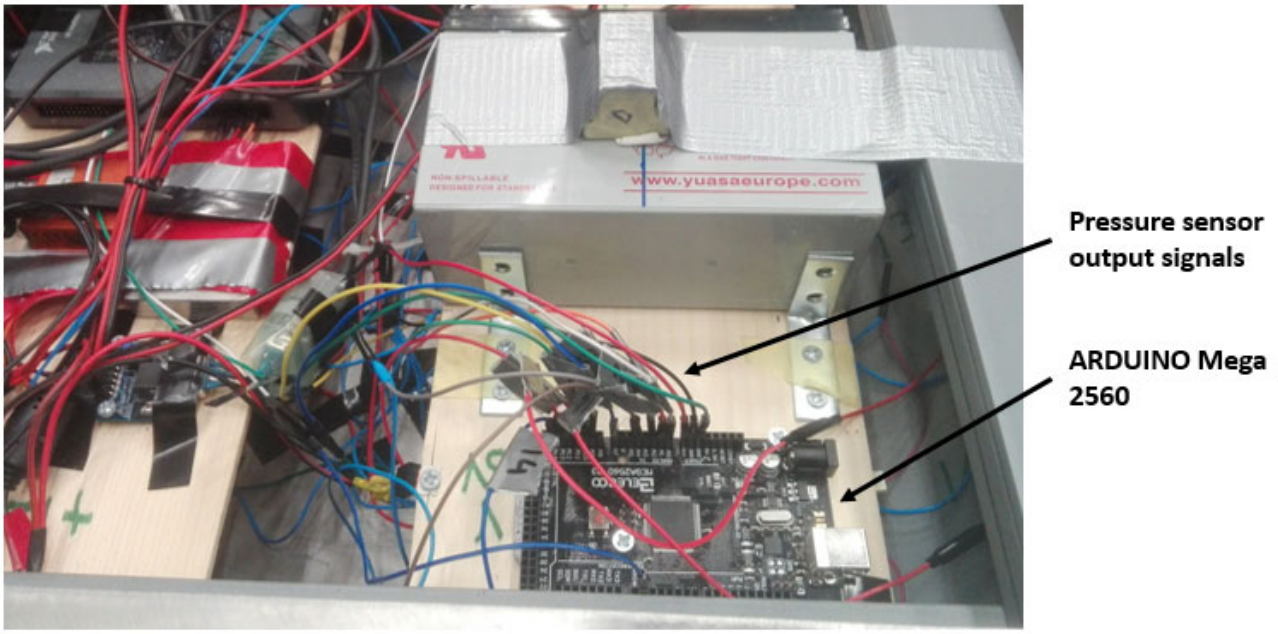

Figure 2-11: ARDUINO Mega 2560 wire connections

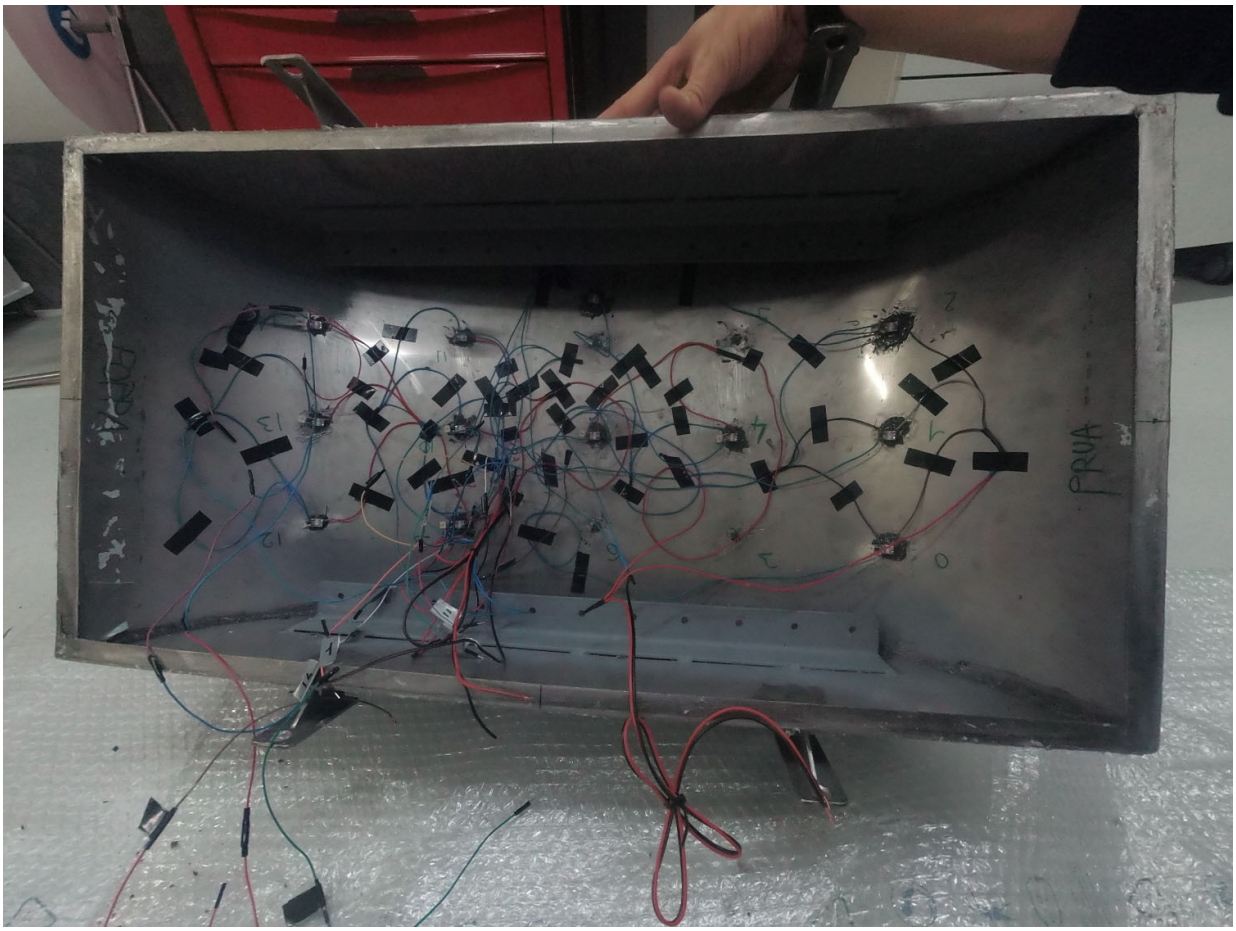

Figure 2-12: Pressure sensor wire connections

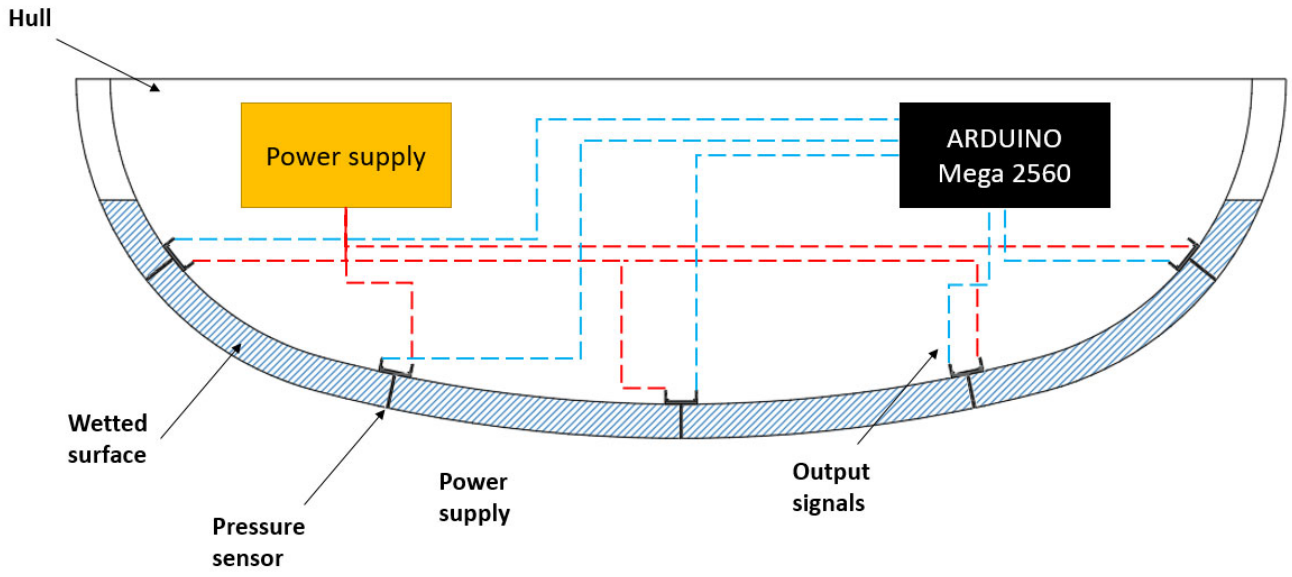

Figure 2-13: Pressure sensors power supply and signal connection

The sensors were acquired using an ARDUINO Mega 2560, which in turn transferred the data via RS232 to UART serial communication to the myRio.

2.1.3 Mooring system and ISWEC deployment

Considering the different mooring configurations suitable for floating WECs, the attention has been focused on slack mooring solutions, because the ISWEC device of interest has a PTO enclosed in the floater and active moorings are not suitable. The ISWEC mooring system is a slack catenary, which corresponds to the SALM (single anchor leg mooring). The next step is to introduce multiple mooring lines. In addition, to guarantee the weathervaning of the device with all the possible wave directions, a proper centre of rotation of the system needs to be designed. The capability of the device to weathervane depends on both the geometry of the hull and the mooring system. Moreover, the ISWEC needs to be connected to the electrical grid with a power transmission cable. To install the electric cable for the grid connection, interference between the cable and the mooring must be avoided while the device is moving. On the other hand, the electric cable must move together with the hull that weathervanes. Hence, the solution requires an electrical slip ring and mechanical swivel to guarantee the correct operation. Figure 2-14 shows the proposed design configuration layout.

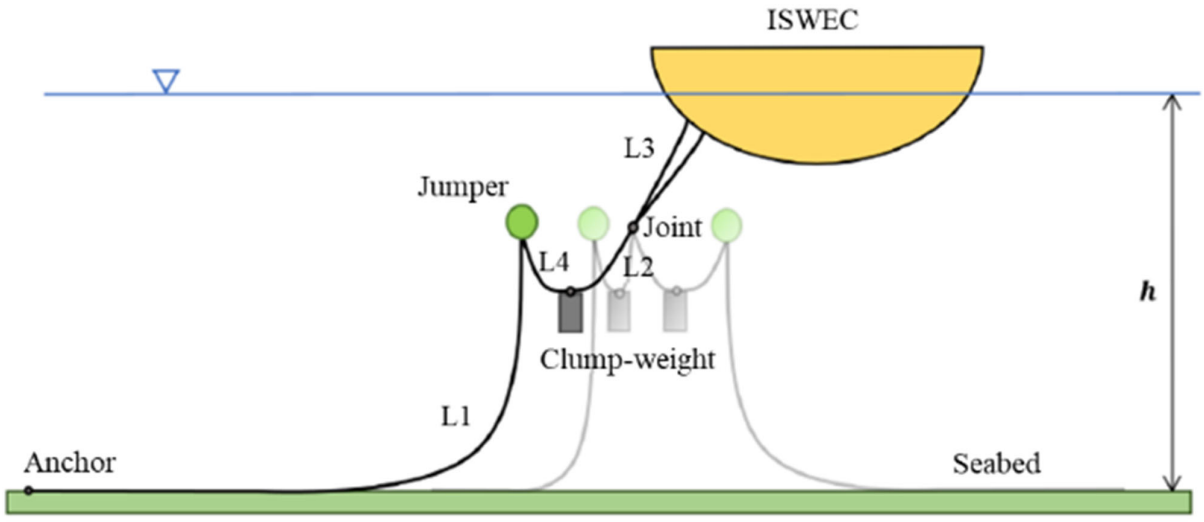

Figure 2-14: ISWEC mooring system configuration

	Scaling factor	1:26 scaled device	Full scale device
Water depth (m)	1	0.96	25
Anchors Positioning radius (m)	1	3	78
L1 (m)	1	3.25	84.5
L2 + L4 (m)	1	0.750	18.5
L3 (m)	1	0.5	13
L1, L2, L4 Nominal diameter (m)	1	0.003	0.078
L3 Nominal diameter (m)	1	0.0022	0.057
L1, L2, L4 mass (kg/m)	3	0.186	125.7
L3 mass (kg/m)	3	0.09	54.080
L1 spring stiffness (N/mm)	2	10	-
L2+L4 spring stiffness (N/mm)	2	43.2	-
L3 spring stiffness (N/mm)	2	34.8	-
L1 Equivalent stiffness (kN/m)	2	9.58	6480
L2+L4 Equivalent stiffness (kN/m)	2	21.78	14729
L3 Equivalent stiffness (kN/m)	2	124.61	84240
L1, L2, L4 Proof load (kN)	3	0.243	3160
L3 Proof load (kN)	3	0.135	1810
L1, L2, L4 Breaking load (kN)	3	0.346	4500
L3 Breaking load (kN)	3	0.193	2600
Jumper net buoyancy (kg)	3	0.44	7733.44
Clump weight (kg)	3	0.250	4394.00

Table 2-2: Scaled mooring properties

The mooring system is composed of three main catenary lines, anchored to the bottom of the sea and connected to the centre of the circumference through a suitable connecting triplate (according to DNV standards) to a mechanical rotary joint that allows the top of the system to rotate. The ISWEC device is connected to the swivel by means of two hawsers attached to the hull. The chains connected to the two hawsers constitute a bridle that prevents the roll motion of the device. The mooring connection point is placed towards the bow, with respect to the centre of gravity of the device, in order to guarantee a lever arm that stabilizes the device at yaw and guarantees the alignment. On each of the bottom catenary a buoyancy component (jumper) is installed to enhance the elastic recall to the system and avoid snatches. At the bottom part of the slip ring the first part of the submarine cable will be attached in the full scale solution. This configuration allows to guide the cable, avoiding bending and tensile stresses and interference with the mechanical components of the system. Moreover, a clump-weight is introduced on each of the three mooring bottom lines. This configuration has been realized to test the effect of the clump-weight on the restoring force of the mooring system and the load peaks reduction in the dynamic behaviour. The main properties of this mooring configuration are listed in Table 2-2.

In order to guarantee the scalability of the loads obtained during the tests and to guarantee an elastic behaviour of the chain compared with the one in the full-scale system, it was necessary to scale the axial stiffness of the mooring lines. When the mooring line is completely taut, the resulting loads depend on the axial stiffness of the line itself. Since the design of the mooring does not depend on the operating conditions in which the device will work but is closely linked to the loads to which it is subjected in extreme sea conditions, it was necessary to scale the axial stiffness. To do this, springs have been introduced in the various sections of the chain in order to obtain a stiffness in scale with respect to the one obtained in the full-scale mooring chain. As shown in Figure 2-17, springs have been introduced in all the chain sections.

In this mooring system, the most critical component, from the system continuity point of view, is the rotating joint. Indeed, it is a single component that connects the upper part of the mooring with the bottom one and failure of this component must be avoided. Moreover, both electrical and mechanical functions are integrated in it. Indeed, for the ISWEC mooring design, attention will be paid on the loads sustained by the joint. In this regard a load cell has been introduced on the central joint (Figure 2-15). A FUTEK LSB210 load cell was chosen. This sensor

is submersible and miniaturized in order to not influence the dynamics of the mooring system. An house-build conditioner has been provided by the wave basin and used to amplify and filter the load cell signal.

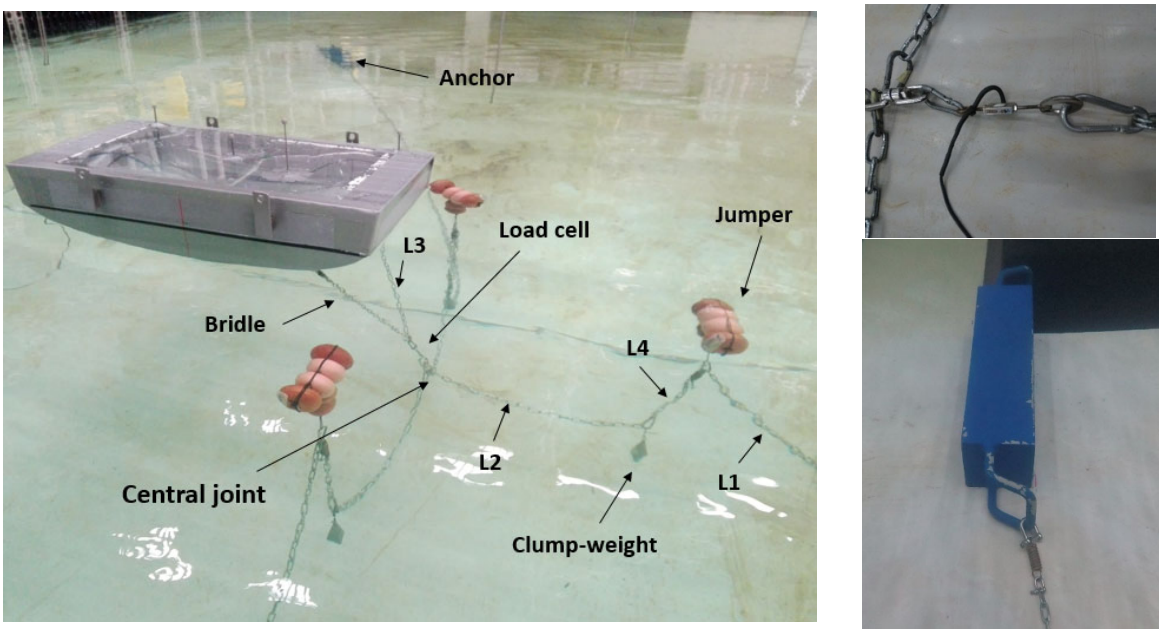

Figure 2-15: ISWEC mooring system main components (lines, load cell and anchor)

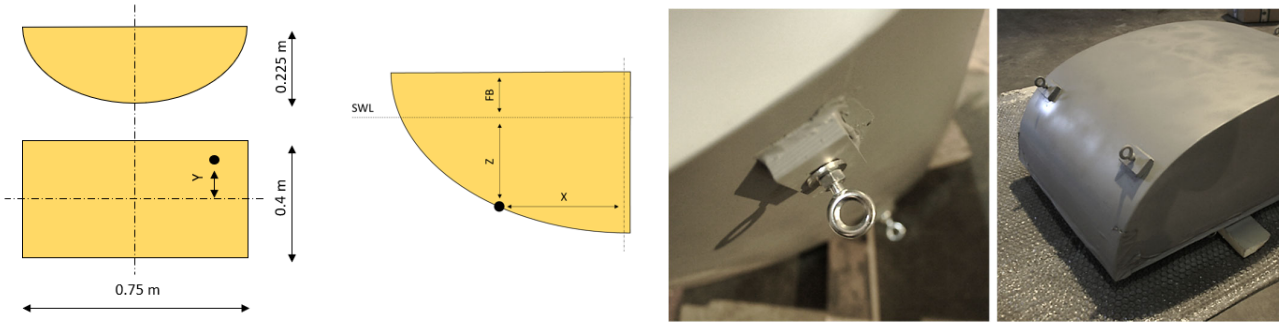

Figure 2-16: Mooring connection points on the hull

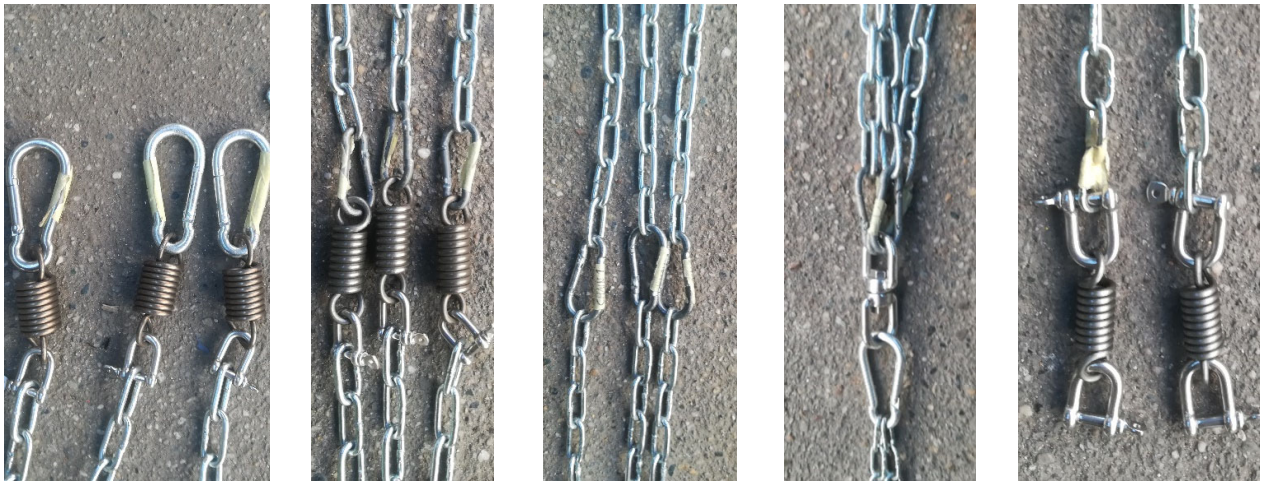

Anchor points (start of L1) | Jumper connection (end of L1 – start of L4) | Clump-weight connection (end of L4 – start of L2) | Central joint (end of L2 – start of L3) | Hull connection (end of L3)

Figure 2-17: Mooring chain connection points

Once the connections with the mooring system were completed, the system was anchored to the wave tank seabed as shown in the Figure 2-18.

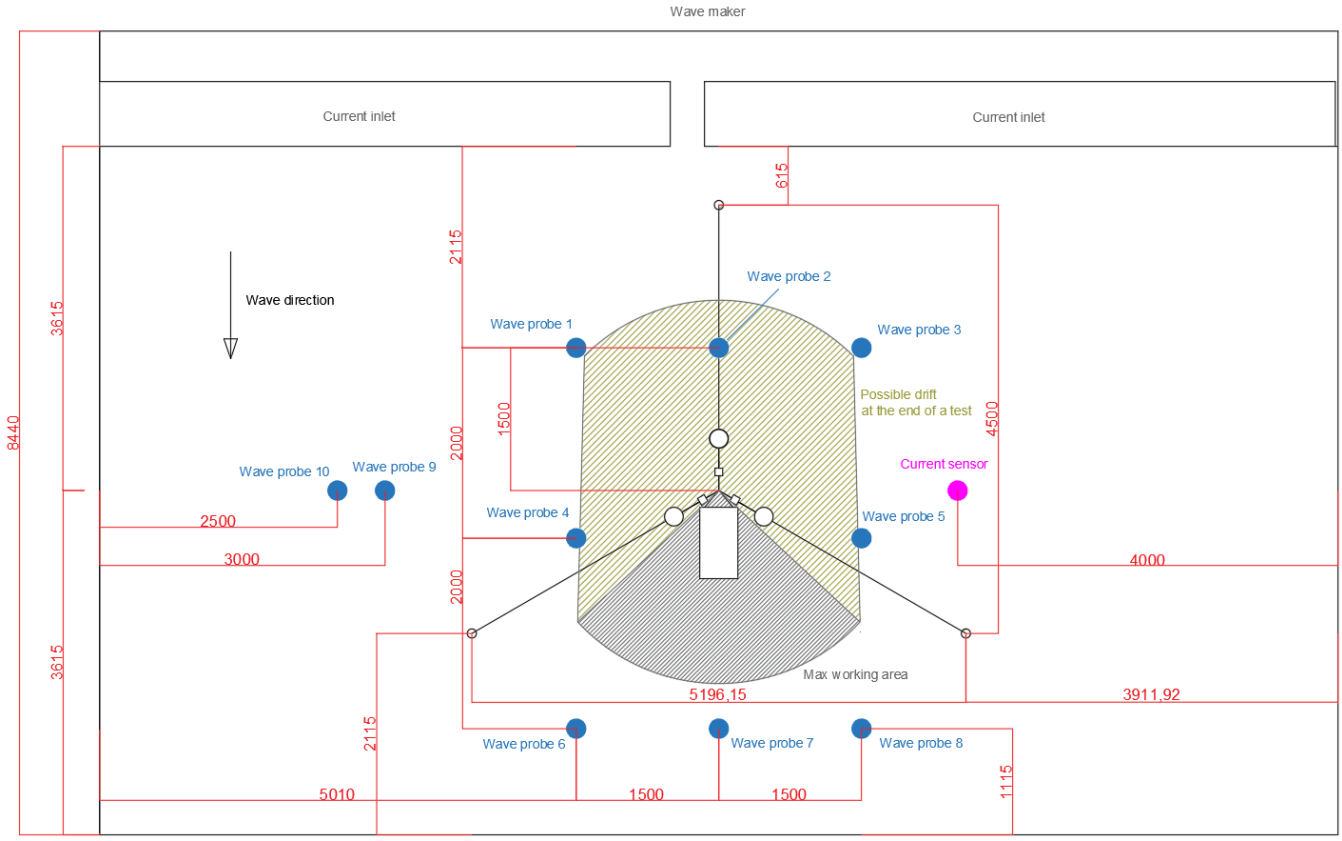

Figure 2-18: CAD scheme of the current sensor, wave gauges positions and ISWEC device deployment

2.1.4 Wave basin and ISWEC acquisition scheme

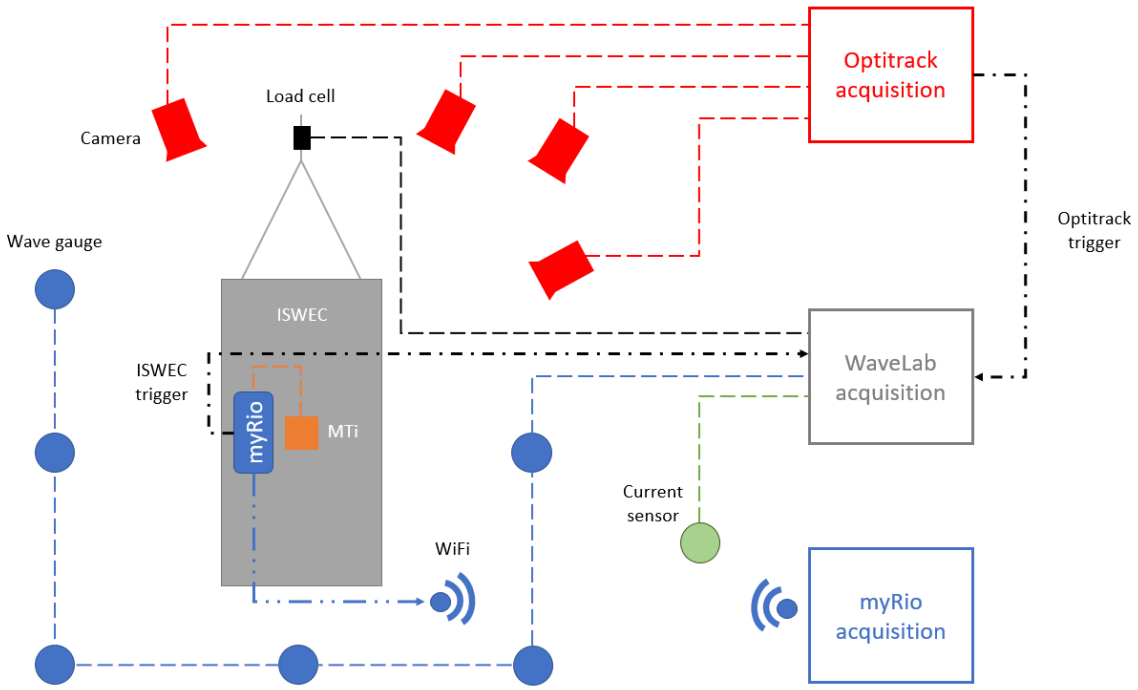

Figure 2-19: Acquisition and synchronization

Referring to the Figure 2-19, the diagram and connection of the sensors used and the acquisition systems is shown. Starting from the ISWEC OnBoard acquisition system, it is represented by the myRIo, which acquires the data coming from the accelerometer (MTi) at a sampling rate of 25 Hz. Through an OffBoard PC, it is possible to control the acquisition of the myRio and download the files saved on it directly to a PC. In addition, the myRio sends a 0-5V digital signal to the WaveLab acquisition system in order to synchronize the acquisition files in post-processing. The Optitrack system acquires the kinematics of the device by means of four cameras that send the signal to an OffBoard PC that reconstructs the motion in the 6 degrees of freedom of the hull. This Optitrack acquisition system also sends a trigger signal to the WaveLab system to synchronize the files acquired in post-processing. Optitrack's data acquisition frame rate is adjustable via software: 25 fps (frame per second) was used. The WaveLab system acquired the 10 wave gauges signals, the current sensor, the load cell and the trigger signals using a NI USB 6225. The acquisition frequency was 100 Hz. Through this system it was possible to calibrate the wave gauges and the current sensor, obtaining the calibration curve for each sensor.

2.2 Tests

The following table summarises the tests carried out:

Name	Tp (s)	Hs (mm)	g	s	dir	Current dir	Device?
REG_T0902_H0025	**0.902**	**0.025**		0	0°	0°	No
REG_T0981_H0030	**0.981**	**0.030**		0	0°	0°	No
REG_T1059_H0035	**1.059**	**0.035**		0	0°	0°	No
REG_T11375_H00404	**1.137**	**0.040**		0	0°	0°	No
REG_T12159_H00462	**1.216**	**0.046**		0	0°	0°	No
REG_T12944_H00523	**1.294**	**0.052**		0	0°	0°	No
REG_T13728_H00588	**1.373**	**0.059**		0	0°	0°	No
REG_T14513_H00658	**1.451**	**0.066**		0	0°	0°	No
REG_T15297_H00731	**1.530**	**0.073**		0	0°	0°	No
IRR_Tp11767_Hs00577_g33_s489_dir0_Cs0_Cd0	**1.177**	**0.058**	3,3	10	0°	0°	No
IRR_Tp13728_Hs00962_g33_s489_dir0_Cs0_Cd0	**1.373**	**0.096**	3,3	10	0°	0°	No
IRR_Tp11512_Hs00673_g33_s489_dir0_Cs0_Cd0	**1.151**	**0.067**	3,3	10	0°	0°	No
IRR_Tp11512_Hs00673_g33_s0_dir0_Cs0_Cd0	**1.151**	**0.067**	3,3	0	0°	0°	No
IRR_Tp13728_Hs00962_g33_s0_dir0_Cs0_Cd0	**1.373**	**0.096**	3,3	0	0°	0°	No
IRR_Tp11512_Hs00673_g33_s0_dir0_Cs0_Cd0	**1.151**	**0.067**	3,3	0	0°	0°	No
EXT_Tp26486_Hs03308_g33_s227_dir0_Cs0_Cd0	**2.648**	**0.331**	3,3	50	0°	0°	No
IRR_Tp11767_Hs00577_g33_s10_dir0_Cs0_Cd0	**1.177**	**0.058**	3,3	10	0°	0°	Yes
IRR_Tp11512_Hs00673_g33_s10_dir0_Cs0_Cd0	**1.151**	**0.067**	3,3	10	0°	0°	Yes
IRR_Tp13728_Hs00962_g33_s10_dir0_Cs0_Cd0	**1.373**	**0.096**	3,3	10	0°	0°	Yes
EXT_Tp24515_Hs02808_g33_s50_dir0_Cs0_Cd0	**2.451**	**0.281**	3,3	50	0°	0°	No
EXT_Tp26083_Hs03192_g33_s50_dir0_Cs0_Cd0	**2.608**	**0.319**	3,3	50	0°	0°	No
EXT_Tp26083_Hs03192_g33_s50_dir0_Cs0_Cd0	**2.608**	**0.319**	3,3	50	0°	0°	Yes
EXT_Tp26083_Hs03192_g33_s50_dir0_Cs0_Cd0	**2.608**	**0.319**	3,3	50	0°	0°	Yes
EXT_Tp26083_Hs03192_g33_s50_dir0_Cs0_Cd0	**2.608**	**0.319**	3,3	50	0°	0°	Yes
EXT_Tp26083_Hs03192_g33_s50_dir0_Cs0_Cd0	**2.608**	**0.319**	3,3	50	0°	0°	Yes
EXT_Tp26083_Hs03192_g33_s50_dir0_Cs0_Cd0	**2.608**	**0.319**	3,3	50	0°	0°	Yes
EXT_Tp26083_Hs03192_g33_s50_dir0_Cs0_Cd0	**2.608**	**0.319**	3,3	50	0°	0°	Yes
EXT_Tp26083_Hs03192_g33_s50_dir0_Cs0_Cd0	**2.608**	**0.319**	3,3	50	0°	0°	Yes
EXT_Tp26083_Hs03192_g33_s50_dir0_Cs0_Cd0	**2.608**	**0.319**	3,3	50	0°	0°	Yes
EXT_Tp26083_Hs03192_g33_s50_dir0_Cs0_Cd0	**2.608**	**0.319**	3,3	50	0°	0°	Yes
EXT_Tp26083_Hs03192_g33_s50_dir0_Cs0_Cd0	**2.608**	**0.319**	3,3	50	0°	0°	Yes

EXT_Tp26083_Hs03192_g33_s50_dir0_Cs0_Cd0	**2.608**	**0.319**	3,3	50	0°	0°	Yes
EXT_Tp26083_Hs03192_g33_s50_dir0_Cs0_Cd0	**2.608**	**0.319**	3,3	50	0°	0°	Yes
EXT_Tp26083_Hs03192_g33_s50_dir0_Cs0_Cd0	**2.608**	**0.319**	3,3	50	0°	0°	Yes
EXT_Tp26083_Hs03192_g33_s50_dir0_Cs0_Cd0	**2.608**	**0.319**	3,3	50	0°	0°	Yes
EXT_Tp26083_Hs03192_g33_s50_dir0_Cs0_Cd0	**2.608**	**0.319**	3,3	50	0°	0°	Yes
REG_T0902_H0025_pressure	**0.902**	**0.025**		0	0°	0°	Yes
REG_T0981_H0030_pressure	**0.981**	**0.030**		0	0°	0°	Yes
REG_T1059_H0035_pressure	**1.059**	**0.035**		0	0°	0°	Yes
REG_T1137_H0040_pressure	**1.137**	**0.040**		0	0°	0°	Yes
REG_T1216_H0046_pressure	**1.216**	**0.046**		0	0°	0°	Yes
REG_T1294_H0052_pressure	**1.294**	**0.052**		0	0°	0°	Yes
REG_T1373_H0059_pressure	**1.373**	**0.059**		0	0°	0°	Yes
REG_T1451_H0066_pressure	**1.451**	**0.066**		0	0°	0°	Yes
REG_T1530_H0073_pressure	**1.530**	**0.073**		0	0°	0°	Yes
REG_T1608_H0081_pressure	**1.608**	**0.081**		0	0°	0°	Yes
REG_T1098_H0038_pressure	**1.098**	**0.038**		0	0°	0°	Yes
REG_T1177_H0043_pressure	**1.177**	**0.043**		0	0°	0°	Yes
REG_T0902_H0036_pressure	**0.902**	**0.036**		0	0°	0°	Yes
REG_T0981_H0043_pressure	**0.981**	**0.043**		0	0°	0°	Yes
REG_T1059_H0050_pressure	**1.059**	**0.050**		0	0°	0°	Yes
REG_T1098_H0054_pressure	**1.098**	**0.054**		0	0°	0°	Yes
REG_T1137_H0058_pressure	**1.137**	**0.058**		0	0°	0°	Yes
REG_T1177_H0062_pressure	**1.177**	**0.062**		0	0°	0°	Yes
REG_T1216_H0066_pressure	**1.216**	**0.066**		0	0°	0°	Yes
REG_T1294_H0075_pressure	**1.294**	**0.075**		0	0°	0°	Yes
REG_T1373_H0084_pressure	**1.373**	**0.084**		0	0°	0°	Yes
REG_T1451_H0094_pressure	**1.451**	**0.094**		0	0°	0°	Yes
REG_T1530_H0104_pressure	**1.530**	**0.104**		0	0°	0°	Yes
REG_T1608_H0115_pressure	**1.608**	**0.115**		0	0°	0°	Yes
IRR_Tp1177_Hs0058_g33_s0_dir0_Cs0_Cd0	**1.177**	**0.058**	3,3	0	0°	0°	Yes
IRR_Tp1372_Hs0096_g33_s0_dir0_Cs0_Cd0	**1.373**	**0.096**	3,3	0	0°	0°	Yes
IRR_Tp1151_Hs0067_g33_s0_dir0_Cs0_Cd0	**1.151**	**0.067**	3,3	0	0°	0°	Yes
IRR_Tp1667_Hs0142_g33_s0_dir0_Cs0_Cd0	**1.667**	**0.142**	3,3	0	0°	0°	Yes
IRR_Tp1314_Hs0077_g33_s0_dir0_Cs0_Cd0	**1.314**	**0.077**	3,3	0	0°	0°	Yes
IRR_Tp1024_Hs0077_g33_s0_dir0_Cs0_Cd0	**1.024**	**0.077**	3.3	0	0°	0°	Yes
IRR_Tp1177_Hs0058_g33_s0_dir30_Cs0_Cd0	**1.177**	**0.058**	3.3	0	30°	0°	Yes
IRR_Tp1372_Hs0096_g33_s0_dir30_Cs0_Cd0	**1.373**	**0.096**	3.3	0	30°	0°	Yes
IRR_Tp1024_Hs0077_g33_s0_dir30_Cs0_Cd0	**1.024**	**0.077**	3.3	0	30°	0°	Yes
IRR_Tp1667_Hs0142_g33_s0_dir0_Cs0_Cd0	**1.667**	**0.142**	3.3	0	0°	0°	Yes
IRR_Tp1024_Hs0077_g33_s0_dir0_Cs0_Cd0	**1.024**	**0.077**	3.3	0	0°	0°	Yes
IRR_Tp1314_Hs0077_g33_s0_dir0_Cs0_Cd0	**1.314**	**0.077**	3.3	0	0°	0°	Yes
IRR_Tp1667_Hs0142_g33_s0_dir30_Cs0_Cd0	**1.667**	**0.142**	3.3	0	30°	0°	Yes
IRR_Tp1024_Hs0058_g33_s0_dir0_Cs0_Cd0	**1.024**	**0.058**	3.3	0	0°	0°	Yes
IRR_Tp1024_Hs0077_g33_s10_dir0_Cs0_Cd0	**1.024**	**0.077**	3.3	10	0°	0°	Yes
IRR_Tp1024_Hs0077_g33_s10_dir30_Cs0_Cd0	**1.024**	**0.077**	3.3	10	30°	0°	Yes
IRR_Tp1373_Hs0096_g33_s10_dir0_Cs0_Cd0	**1.373**	**0.096**	3.3	10	0°	0°	Yes

IRR_Tp1373_Hs0096_g33_s10_dir30_Cs0_Cd0	**1.373**	**0.096**	3.3	10	30°	0°	Yes
REG_T0941_H0028_pressure	**0.941**	**0.028**		0	0°	0°	Yes
REG_T1024_H0033_pressure	**1.024**	**0.033**		0	0°	0°	Yes
REG_T0941_H0040_pressure	**0.941**	**0.040**		0	0°	0°	Yes
REG_T1024_H0047_pressure	**1.024**	**0.047**		0	0°	0°	Yes
REG_T0863_H0023_pressure	**0.863**	**0.023**		0	0°	0°	Yes
REG_T0863_H0033_pressure	**0.863**	**0.033**		0	0°	0°	Yes
IRR_Tp1177_Hs0058_g33_s0_dir30_CsMax_Cd0	**1.177**	**0.058**	3.3	0	30°	0°	Yes
IRR_Tp1373_Hs0096_g33_s0_dir30_CsMax_Cd0	**1.373**	**0.096**	3.3	0	30°	0°	Yes
IRR_Tp1024_Hs0077_g33_s0_dir30_CsMax_Cd0	**1.024**	**0.077**	3.3	0	30°	0°	Yes
IRR_Tp1667_Hs0142_g33_s0_dir30_CsMax_Cd0	**1.667**	**0.142**	3.3	0	30°	0°	Yes
EXT_Tp2608_Hs0319_g33_s50_dir0_Cs0_Cd0	**2.608**	**0.319**		50	0°	0°	Yes

Table 2-3: Wave test program

2.3 Results

This section describes the results obtained by the experimental campaign, showing the critical aspects of the analysis of the results as well as the results themselves.

2.3.1 Wave gauges calibration

Initially, a wave gauges test was performed, generating a series of waves before placing the hull in the water. This was done to verify the correct functioning of the sensors before proceeding with the positioning of the hull.

For what concern regular waves, as shown in tables Table 2-4 and Table 2-5, statistical data were extracted for each wave considering the measured wave height time histories of the wave gauges. To obtain these results, a frequency analysis was performed on the above mentioned time histories. The procedure included a preliminary analysis of the signals in order to choose the time interval for which to perform the Fourier analysis. Once the correct range was found, Fourier analysis was performed, obtaining the peak height and period. Finally, statistical parameters have been calculated for each wave as shown in the tables Table 2-4 and Table 2-5, both for the peak height and period, considering all the 10 wave gauges results.

It can be noticed that for the waves considered all the wave gauges measure about the same value for the peak period. This is not the case for wave height, as statistical parameters show a relevant variance in the values measured by the sensors. Considering for example the wave T=1.215s and H=0.046m, Figure 2-20 shows how the wave height measured by wave gauge 10 is almost the same as the theoretical wave generated both without and with the device.

	Wave data		**Wave height statistical values**				
Name	**T (s)**	**H (m)**	Mean (m)	Standard dev (m)	Variance (m)	Maximal value (m)	Minimal value (m)
REG_T0902_H0025	**0.902**	**0.025**	0.0273	0.0017	$2.95 \cdot 10^{-6}$	0.031	0.0255
REG_T0981_H0030	**0.981**	**0.030**	0.284	0.0050	$2.53 \cdot 10^{-5}$	0.0336	0.0208
REG_T1059_H0035	**1.059**	**0.035**	0.0364	0.0035	$1.24 \cdot 10^{-5}$	0.043	0.0317
REG_T11375_H00404	**1.137**	**0.040**	0.0423	0.0056	$3.15 \cdot 10^{-5}$	0.0469	0.0317
REG_T12159_H00462	**1.216**	**0.046**	0.0439	0.0057	$3.28 \cdot 10^{-5}$	0.0517	0.0359
REG_T12944_H00523	**1.294**	**0.052**	0.0498	0.0051	$2.57 \cdot 10^{-5}$	0.0578	0.0392
REG_T13728_H00588	**1.373**	**0.059**	0.0536	0.0108	$1.17 \cdot 10^{-4}$	0.0674	0.0376
REG_T14513_H00658	**1.451**	**0.066**	0.0638	0.0087	$7.64 \cdot 10^{-5}$	0.0752	0.0528
REG_T15297_H00731	**1.530**	**0.073**	0.0665	0.0064	$4.03 \cdot 10^{-5}$	0.0753	0.0573

Table 2-4 Regular wave statistical data – focus on wave height

	Wave data		Wave period statistical values				
Name	**T (s)**	**H (m)**	Mean (s)	Standard dev (s)	Variance (s)	Maximal value (s)	Minimal value (s)
REG_T0902_H0025	**0.902**	**0.025**	0.9025	$6.94 \cdot 10^{-4}$	$4.80 \cdot 10^{-7}$	0.9036	0.9015
REG_T0981_H0030	**0.981**	**0.030**	0.9811	$1.93 \cdot 10^{-4}$	$3.70 \cdot 10^{-8}$	0.9813	0.9807
REG_T1059_H0035	**1.059**	**0.035**	1.0592	$3.03 \cdot 10^{-4}$	$9.18 \cdot 10^{-8}$	1.0595	1.0585
REG_T11375_H00404	**1.137**	**0.040**	1.1377	$6.21 \cdot 10^{-4}$	$3.86 \cdot 10^{-7}$	1.1383	1.1363
REG_T12159_H00462	**1.216**	**0.046**	1.216	$3.35 \cdot 10^{-4}$	$1.12 \cdot 10^{-7}$	1.2167	1.2158
REG_T12944_H00523	**1.294**	**0.052**	1.294	$6.74 \cdot 10^{-4}$	$4.54 \cdot 10^{-7}$	1.2953	1.2933
REG_T13728_H00588	**1.373**	**0.059**	1.3730	$6.11 \cdot 10^{-4}$	$3.73 \cdot 10^{-7}$	1.3739	1.3719
REG_T14513_H00658	**1.451**	**0.066**	1.4515	$7.84 \cdot 10^{-4}$	$6.15 \cdot 10^{-7}$	1.4525	1.4504
REG_T15297_H00731	**1.530**	**0.073**	1.5299	$6.02 \cdot 10^{-4}$	$3.62 \cdot 10^{-7}$	1.5306	1.5288

Table 2-5 Regular wave statistical data – focus on wave period

	Wave data		Wave period results		Wave height results	
Wave gauges	**T (s)**	**H (m)**	T measured (s)	T error (%)	H measured (m)	H error (%)
Wave gauge 1	**1.215**	**0.046**	1.216	-0.02	0.042	-9.02
Wave gauge 2	**1.215**	**0.046**	1.217	0.08	0.045	-3.24
Wave gauge 3	**1.215**	**0.046**	1.216	0.01	0.041	-11.42
Wave gauge 4	**1.215**	**0.046**	1.216	0.04	0.038	-18.73
Wave gauge 5	**1.215**	**0.046**	1.216	0.02	0.036	-22.15
Wave gauge 6	**1.215**	**0.046**	1.216	-0.01	0.05	8.87
Wave gauge 7	**1.215**	**0.046**	1.216	0	0.039	-16.34
Wave gauge 8	**1.215**	**0.046**	1.216	-0.02	0.0520	11.95
Wave gauge 9	**1.215**	**0.046**	1.216	0.02	0.0480	3.96
Wave gauge 10	**1.215**	**0.046**	1.216	0.02	0.048	4.97

Table 2-6 Wave probes frequency domain analysis. Regular wave data: T=1.215s and H=0.046m. No device.

	Wave data		Wave period results		Wave height results	
Wave gauges	**T (s)**	**H (m)**	T measured (s)	T error (%)	H measured (m)	H error (%)
Wave gauge 1	**1.215**	**0.046**	1.216	0.07	0.039	-13.83
Wave gauge 2	**1.215**	**0.046**	1.218	0.21	0.044	-4.31
Wave gauge 3	**1.215**	**0.046**	1.217	0.09	0.041	-10.82
Wave gauge 4	**1.215**	**0.046**	1.217	0.09	0.037	-18.68
Wave gauge 5	**1.215**	**0.046**	1.216	0.04	0.039	-14.70
Wave gauge 6	**1.215**	**0.046**	1.216	0.07	0.048	5.38
Wave gauge 7	**1.215**	**0.046**	1.218	0.18	0.038	-16.02
Wave gauge 8	**1.215**	**0.046**	1.216	0.02	0.049	7.15
Wave gauge 9	**1.215**	**0.046**	1.216	0.05	0.054	17.75
Wave gauge 10	**1.215**	**0.046**	1.216	0.07	0.049	7.788

Table 2-7 Wave probes frequency domain analysis. Regular wave data: T=1.215s and H=0.046m. With device.

Wave probe 10 and 9 are the sensors that will be considered undisturbed by the effects of reflection and radiation of the hulls and therefore the results obtained will refer to them. However, comparing the results of the wave gauge data showed in Table 2-6 and Table 2-7, it can be noticed that the wave gauge 9 is not totally undisturbed. In fact, referring to Table 2-6 (test without the device) its percentage difference in term of wave height measured with respect to the theoretical wave height is lower compared with the result reported in Table 2-7 (test without the device).

For what concern irregular waves, a statistical analysis was performed for five waves with different input data. Statistical data were extracted for each wave considering the measured wave height time histories of the wave probes. All the waves were generated considering a Jonswap spectrum with a gamma coefficient equal to 3.3, different peak period and significant wave height, and different spread factor (multidirectional waves). The wave

tank was able to generate even irregular wave spectra by varying the spread factor. This parameter allows you to spread the power of the wave generated at a certain angle, defined by the spread parameter. This allows obtaining a wave more similar to a real wave and therefore allowing the evaluation of the device in conditions more similar to the operating conditions in which it will work.

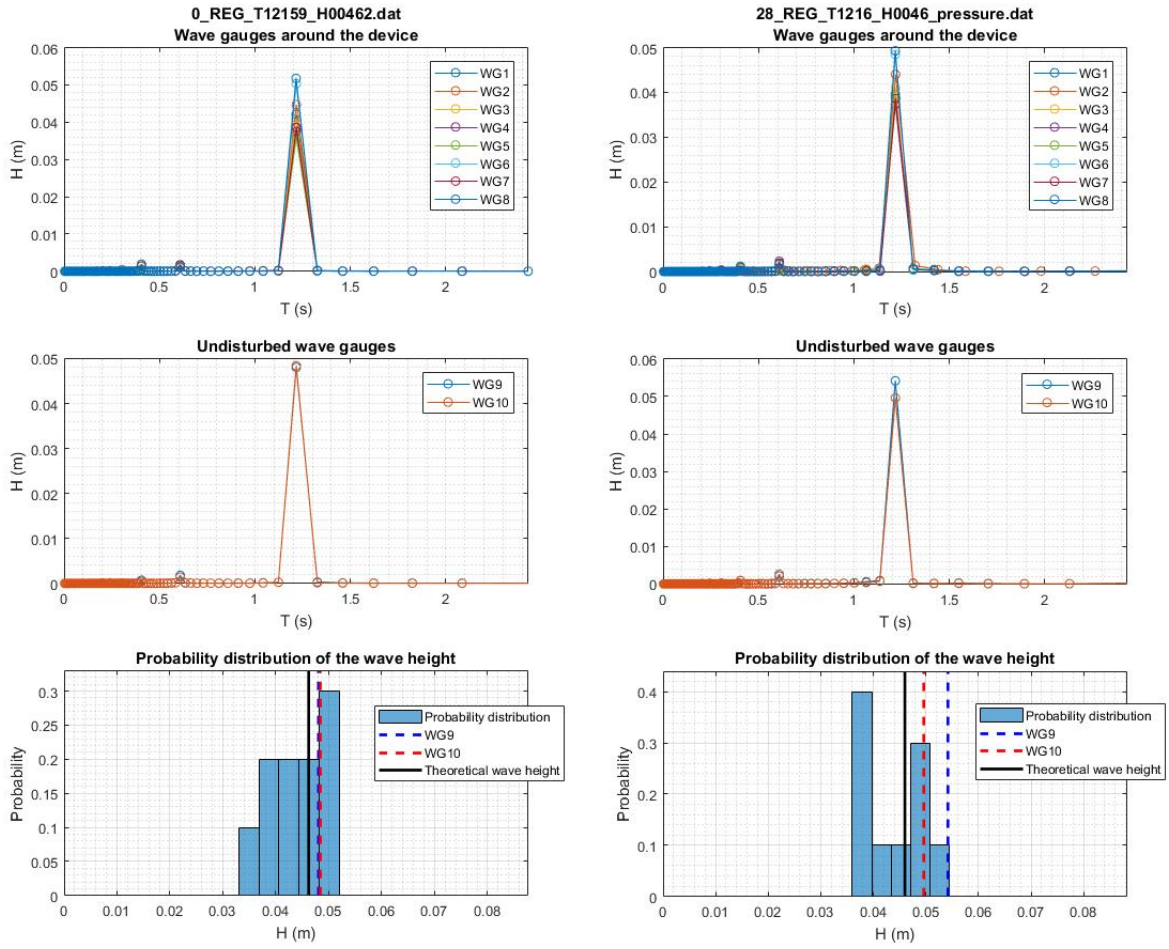

Figure 2-20: FFT analysis and statistical distribution of the wave height. Regular wave data: T=1.059s and H=0.035m. No device (left) vs With device (right)

The procedure included a preliminary analysis of the signals in order to determine the time interval for which to perform the frequency domain analysis. Once the correct range was found, frequency domain analysis was performed by means of the Welch method, obtaining the significant wave height and energy period. Finally, statistical parameters have been calculated for each wave as shown in Table 2-8 and Table 2-9, both for the significant wave height and energy period.

	Wave data				Wave significant height statistical values		
Name	**Tp (s)**	**Hs (m)**	γ	**s**	Mean (m)	Standard dev (m)	Variance (m)
IRR_Tp11767_Hs00577_g33_s489_dir0_Cs0_Cd0	**1,177**	**0,058**	3,3	10	0.0579	0.0012	$1.50 \cdot 10^{-6}$
IRR_Tp13728_Hs00962_g33_s489_dir0_Cs0_Cd0	**1,373**	**0,096**	3,3	10	0.0926	0.0029	$8.30 \cdot 10^{-6}$
IRR_Tp11512_Hs00673_g33_s489_dir0_Cs0_Cd0	**1,151**	**0,067**	3,3	10	0.0656	0.0022	$4.74 \cdot 10^{-6}$
IRR_Tp11512_Hs00673_g33_s0_dir0_Cs0_Cd0	**1,151**	**0,067**	3,3	0	0.0695	0.0019	$3.72 \cdot 10^{-6}$
IRR_Tp13728_Hs00962_g33_s0_dir0_Cs0_Cd0	**1,373**	**0,096**	3,3	0	0.0932	0.0040	$1.56 \cdot 10^{-5}$

Table 2-8 Irregular wave statistical data – focus on significant wave height

	Wave data				Wave significant period statistical values		
Name	**Tp (s)**	**Hs (m)**	γ	**s**	Mean (s)	Standard dev (s)	Variance (s)
IRR_Tp11767_Hs00577_g33_s489_dir0_Cs0_Cd0	**1,177**	**0,058**	3,3	10	1.1892	0.0173	$2.98 \cdot 10^{-4}$
IRR_Tp13728_Hs00962_g33_s489_dir0_Cs0_Cd0	**1,373**	**0,096**	3,3	10	1.3648	0.0499	0.025
IRR_Tp11512_Hs00673_g33_s489_dir0_Cs0_Cd0	**1,151**	**0,067**	3,3	10	1.1545	0.0302	$9.13 \cdot 10^{-4}$
IRR_Tp11512_Hs00673_g33_s0_dir0_Cs0_Cd0	**1,151**	**0,067**	3,3	0	1.1475	0.0157	$2.46 \cdot 10^{-4}$
IRR_Tp13728_Hs00962_g33_s0_dir0_Cs0_Cd0	**1,373**	**0,096**	3,3	0	1.3936	0.0243	$5.91 \cdot 10^{-4}$

Table 2-9 Irregular wave statistical data – focus on energy period

	Wave data		Wave period results		Wave height results	
Wave gauges	**Tp (s)**	**Hs (m)**	Tp measured (s)	Tp error (%)	Hs measured (m)	Hs error (%)
Wave gauge 1	**1,151**	**0,067**	1,138	-1,170	0,069	2,480
Wave gauge 2	**1,151**	**0,067**	1,138	-1,170	0,068	1,770
Wave gauge 3	**1,151**	**0,067**	1,138	-1,170	0,068	0,940
Wave gauge 4	**1,151**	**0,067**	1,138	-1,170	0,070	3,900
Wave gauge 5	**1,151**	**0,067**	1,138	-1,170	0,073	8,420
Wave gauge 6	**1,151**	**0,067**	1,138	-1,170	0,071	5,260
Wave gauge 7	**1,151**	**0,067**	1,138	-1,170	0,072	6,290
Wave gauge 8	**1,151**	**0,067**	1,170	1,660	0,070	3,800
Wave gauge 9	**1,151**	**0,067**	1,170	1,660	0,068	1,320
Wave gauge 10	**1,151**	**0,067**	1,170	1,660	0,067	-0,220

Table 2-10 Wave probes frequency domain analysis. Irregular wave data: Tp=1.152s and Hs=0.0673m. No device.

	Wave data		Wave period results		Wave height results	
Wave gauges	**Tp (s)**	**Hs (m)**	Tp measured (s)	Tp error (%)	Hs measured (m)	Hs error (%)
Wave gauge 1	**1,151**	**0,067**	1,138	-1,15	0,067	-0,13
Wave gauge 2	**1,151**	**0,067**	1,138	-1,15	0,065	-2,79
Wave gauge 3	**1,151**	**0,067**	1,138	-1,15	0,067	0,10
Wave gauge 4	**1,151**	**0,067**	1,138	-1,15	0,068	0,94
Wave gauge 5	**1,151**	**0,067**	1,138	-1,15	0,072	6,94
Wave gauge 6	**1,151**	**0,067**	1,170	1,68	0,069	2,33
Wave gauge 7	**1,151**	**0,067**	1,138	-1,15	0,062	-7,06
Wave gauge 8	**1,151**	**0,067**	1,170	1,68	0,065	-2,96
Wave gauge 9	**1,151**	**0,067**	1,205	4,67	0,069	2,59
Wave gauge 10	**1,151**	**0,067**	1,205	4,67	0,066	-1,73

Table 2-11 Wave probes frequency domain analysis. Irregular wave data: Tp=1.152s and Hs=0.0673m. With device.

It can be noticed that for the waves considered all the wave gauges measure about the same value for the peak period and significant wave height. Considering the wave 'IRR_Tp11512_Hs00673_g33_s0_dir0_Cs0_Cd0', Figure 2-21 compares the same wave mono directional (figure on the left) with the spread one (figure on the right). It can be noticed that the spread one has a low energetic content in respect to the mono directional one. Considering again the wave 'IRR_Tp11512_Hs00673_g33_s0_dir0_Cs0_Cd0', Figure 2-22, Table 2-10 and Table 2-11 show how the wave spectra of the 'No device' case is almost the same of the 'With device' case for the wave gauge 9 and 10. Moreover, both are almost the same with respect to the theoretical one. This means that the wave gauge 9 and 10 can be considered as undisturbed.

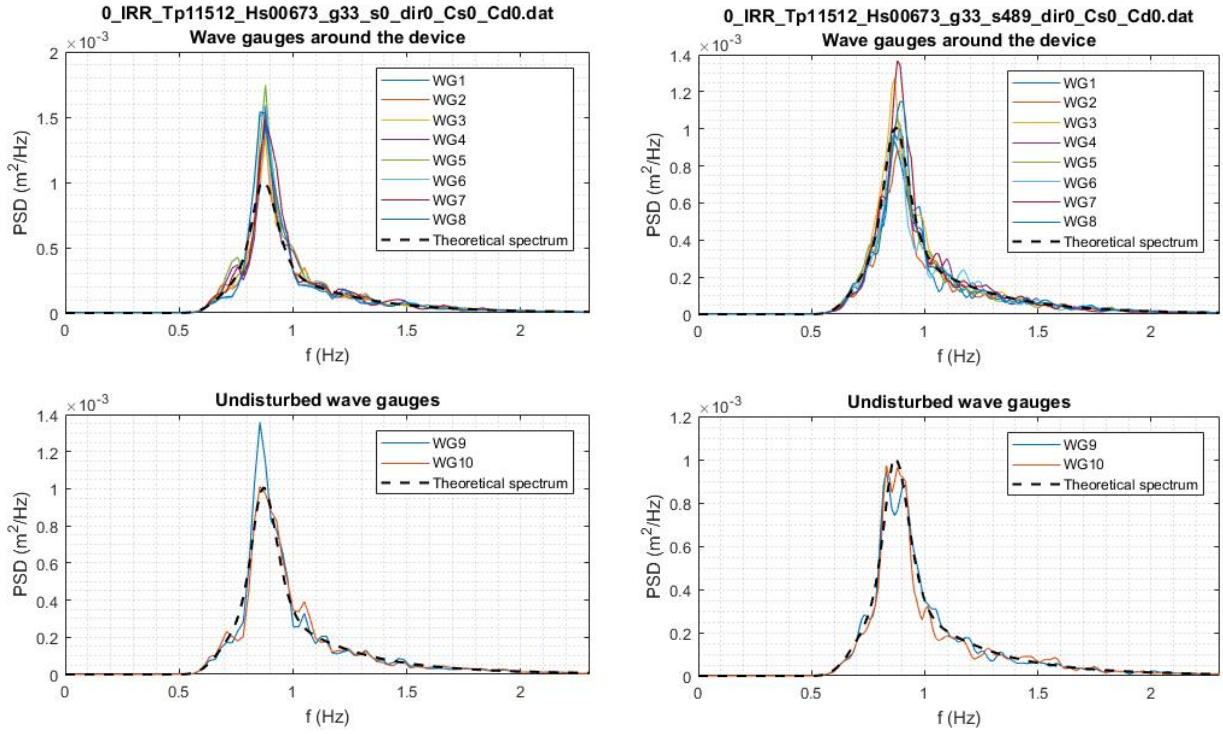

Figure 2-21: Welch analysis of irregular wave, power spectra. Irregular wave data: Tp=1.152s and Hs=0.0673m. Mono directional (left) vs Multi directional (right)

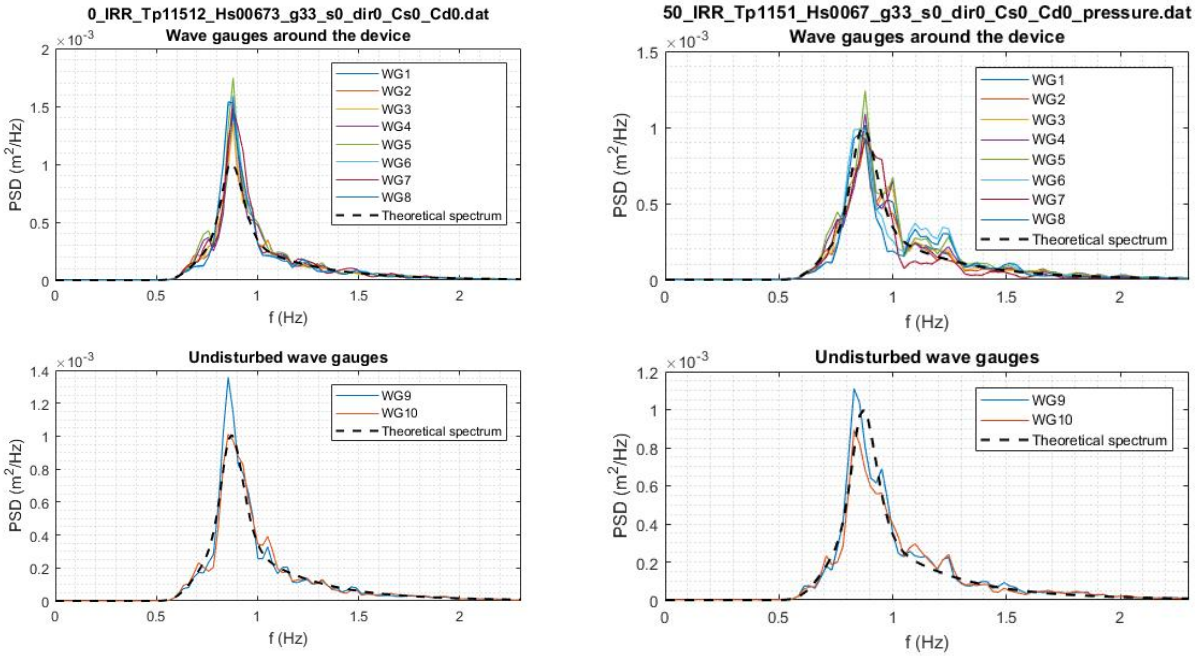

Figure 2-22: Welch analysis of irregular wave, power spectra. Irregular wave data: Tp=1.152s and Hs=0.0673m. No device (left) vs With device (right)

2.3.2 Free decay analysis

Once the deployment of the hull was done as described in the chapter of the experimental setup, several free decay tests were carried out in order to identify the resonance period and the viscous damping coefficient of the scaled device. The acquisition data taken from the free decay tests of ISWEC in pitch are presented in the next figure:

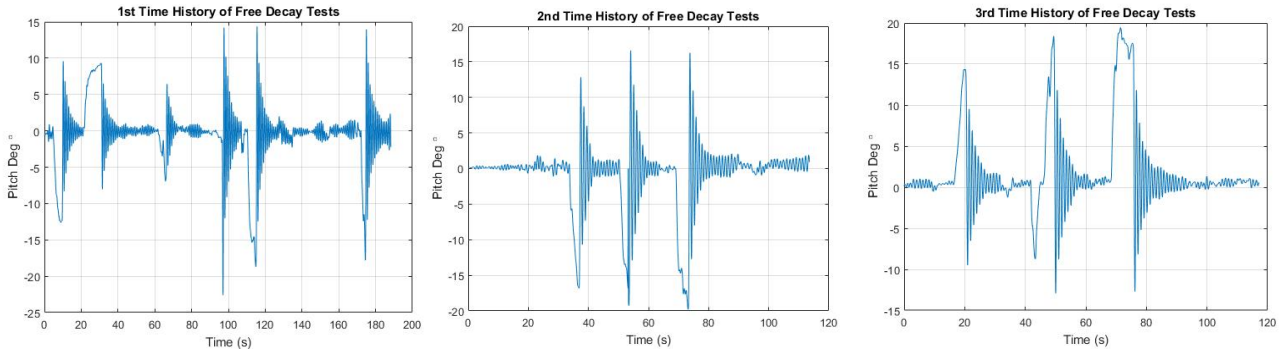

Figure 2-23 Pitch free decay test time histories

As it is presented, during the free decay experiments, ISWEC was initially rotated in a specific angle and afterwards it was released in order to capture the free decay behaviour. In total, 12 free decay experiments took place during the experimental campaign. All the Free Decay Tests were filtered in order to eliminate the existing noise in the dynamic response. Another very important process for the elaboration of the data is the elimination of the mean value or the linear trend from the responses. For the identification of the linear and the non-linear quadratic damping, an identification process from the naval field presented in [7] was applied. The equations presented in Begovic's paper were used in order to identify the damping coefficients during the roll motion of naval ships. However, they can be applied without any problem in the identification of the damping coefficient during the pitch motion of ISWEC. It was assumed that dynamics can be described by a single degree of freedom.

$$(I_{55} + A_{55})\ddot{\phi} + B_{55-total}(\dot{\phi}) + C_{55}\phi = 0 \quad (1)$$

Where:

- I_{55} : Inertia of ISWEC in pitch
- A_{55} : Added mass
- $B_{55-total}$: Total damping term
- C_{55} : Hydrostatic stiffness

The terms of added mass A_{55} and damping $B_{55-total}$ are function of frequency, and in this case, they are related to the natural period of the system. The term of nonlinear damping $B_{55-total}$ can be subdivided and approximated by the sum of two contributions, linear and quadratic:

$$B_{55-total} = B_{55-1}\dot{\phi} + B_{55-2}\dot{\phi}|\dot{\phi}| \quad (2)$$

Writing the equation in a different way:

$$\ddot{\phi} + 2\alpha\dot{\phi} + \beta\dot{\phi}|\dot{\phi}| + \omega_n^2\phi = 0 \quad (3)$$

Where:

- $\alpha = \frac{B_{44-1}}{2(I_{44}+M_{44})}$ is the linear extinction coefficient
- $\alpha = \frac{B_{44-2}}{(I_{44}+M_{44})}$ is the quadratic extinction coefficient
- $\alpha = \frac{B_{44-1}}{2(I_{44}+M_{44})}$ is the cubic extinction coefficient
- $\omega_{\phi 0} = \sqrt{\frac{C_{44}}{I_{44}+M_{44}}}$ is the natural pitch frequency

Linearizing the non-linear term using Fourier series, rewriting it and defining the extinction coefficient we can obtain:

$$\dot{\phi}|\dot{\phi}| \approx \frac{8}{3\pi}\omega_{\phi}\phi_i\phi \quad (4)$$

$$\ddot{\phi} + 2\alpha_{eq}\dot{\phi} + \omega_n^2\phi = 0 \tag{5}$$

$$\alpha_{eq} = \alpha + \frac{4}{3\pi}\omega_\phi\phi_i\beta + \frac{3}{8}\omega_\phi^2\phi_i\beta = \frac{B_{44-total}}{2(I_{44} + A_{44})} \tag{6}$$

The logarithmic decrease is considered:

$$\Delta\phi = ln\left(\frac{|\phi_i|}{|\phi_{i+1}|}\right) \tag{7}$$

$$\alpha_{i-log} \approx \frac{1}{t_{i+1} - t_i} ln\left(\frac{|\phi_i|}{|\phi_{i+1}|}\right) \equiv \alpha + \frac{4}{3\pi}\omega_\phi\phi_{mean-i}\beta \tag{8}$$

$$\phi_{mean} = \frac{|\phi_i| + |\phi_{i+1}|}{2} \tag{9}$$

The natural pitch frequency can be written as:

$$\omega_{\phi 0} = \sqrt{\omega_\phi^2 + \alpha_{eq}^2} \tag{10}$$

From the free decay curves the curve of α_{eq} can be calculated as a function of φ by employing the linear data regression curve in the form:

$$\alpha_{eq} = ax + b \tag{11}$$

Thus, the terms of linear and quadratic extinction are calculated:

$$\alpha = b \tag{12}$$

$$\beta \equiv \frac{3\pi}{4\omega_\phi}a \tag{13}$$

For every Free Decay response, the maximum and minimum peaks have been identified. Figure 2-24 shows the analysis of free pitch decay. The intercept on the y-axis represents the linear damping component. It is noted that the dispersion of data increases as the pitch value decreases. Taking into account the continuous line, we obtain the following values (Table 2-12):

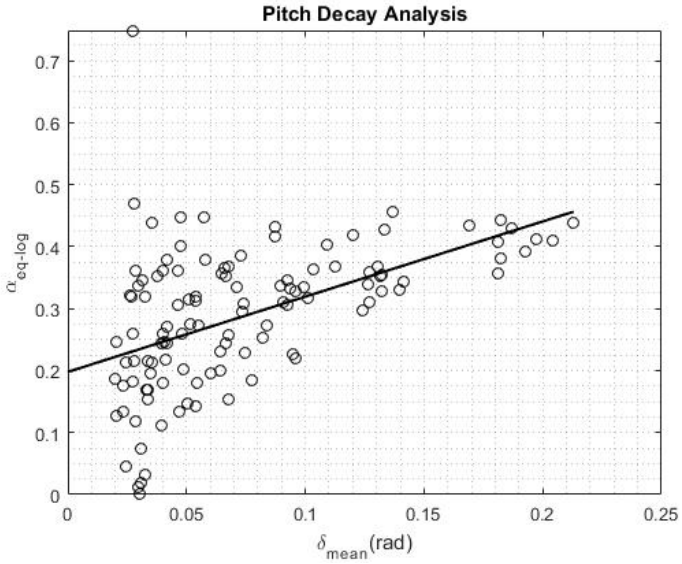

Figure 2-24 Pitch damping coefficient identification

	Free decay Results		
	Natural period (s)	α	β
ISWEC scaled device 1:26	1.024	1.2138	0.1979

Table 2-12 Free decay analysis results

2.3.3 Irregular waves analysis

For what concern irregular waves, a performance analysis of it was performed considering first a monodirectional sea and then a sea with a different spread coefficient (48.9°) and a different direction (30°). The waves were running for more than 10 minutes in order to obtain the development of all the harmonics. In order to compare the performances of the hull for different waves three degrees of freedom were considered: pitch, roll and heave. For each of them, a frequency analysis was carried out using the Welch method.

Referring to Figure 2-25 several consideration can be carried out:

- For what concern the pitch spectrum, it can be noticed that the hull has its peak of energy at the resonance period (equal to 1.024s). This mean that the ISWEC extracts more energy thanks to the wave components close to its resonance frequency despite the fact that the generated wave has a peak of energy at a different frequency.
- The same behaviour is the roll, which has the peak of the energetic content near the roll natural frequency.
- For the heave it is possible to notice how the hull behaves like a low pass filter, perfectly reproducing the PSD of the input wave for the low frequencies and cutting for the high frequencies.
- Moreover, the last chart at the bottom right shows how the undisturbed wave gauges give reliable spectra of the generated wave.

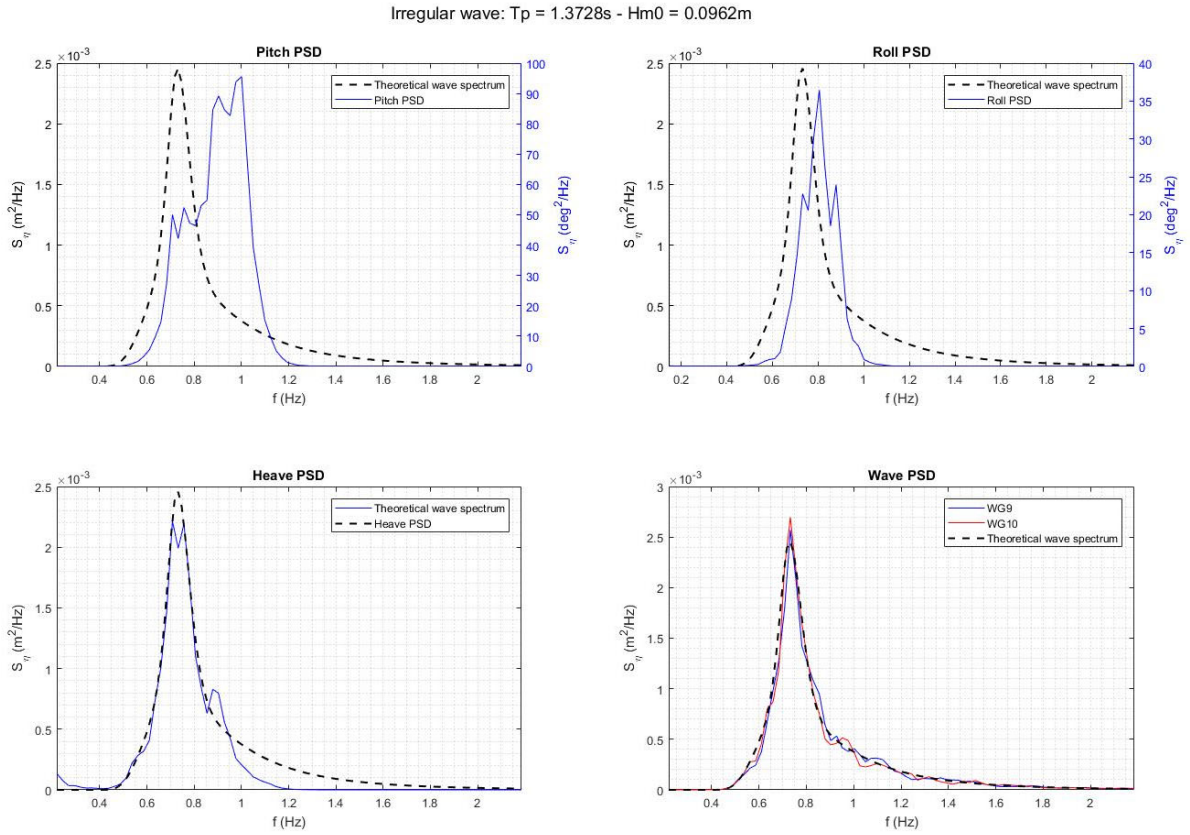

Figure 2-25 Irregular wave analysis. Irregular wave data: Tp=1.3728s and Hm0=0.0962m

Once the behaviour of the hull for an irregular unidirectional wave had been analysed, a more in-depth analysis was carried out for complex sea states. In fact, considering a real sea, it is necessary to consider a multidirectional

sea. That said, different directions and spread factors were tested for the same irregular wave. In this report we report the analysis for the resonance wave.

Referring to Table 2-13 and Figure 2-26 several considerations can be carried out:

- For what concern the pitch spectrum, by increasing the spread coefficient, the rms value of the pitch decreases as the wave energy is more spread. On the contrary, the response of the system is not affected by the direction of the wave: considering a wave at 0 or 30 degrees, the rms value of the pitch does not change and therefore it is possible to conclude how the mooring allows the system to orient itself correctly with the direction of the wave.
- The opposite behaviour is the roll, which increases with the increase of the spread coefficient as the hull is subject to a lateral energy component. Anyway, for what concern the effect of the wave direction, it can be seen that again the wave direction does not affect the hull hydrodynamics.

	Wave data				Pitch results			Roll results		
Name	**Tp (s)**	**Hs (m)**	**Dir (°)**	**S (°)**	rms (°)	max (°)	min (°)	rms (°)	max (°)	min (°)
IRR_Tp1024_Hs0077_g33_s0_dir0	**1.024**	**0.077**	**0**	**0**	6.71	22.32	-20.81	0.53	2.09	-1.96
IRR_Tp1024_Hs0077_g33_s0_dir30	**1.024**	**0.077**	**30**	**0**	7.07	19.56	-19.24	0.99	3.61	-3.36
IRR_Tp1024_Hs0077_g33_s10_dir0	**1.024**	**0.077**	**0**	**48.9**	5.95	21.72	-21.32	1.91	6.00	-6.45
IRR_Tp1024_Hs0077_g33_s10_dir30	**1.024**	**0.077**	**39**	**48.9**	6.41	20.14	-19.42	1.85	5.89	-6.92

Table 2-13 Irregular wave complex sea state analysis, roll and pitch results. Irregular wave data: Irregular wave data: Tp=1.024s and Hm0=0.077m.

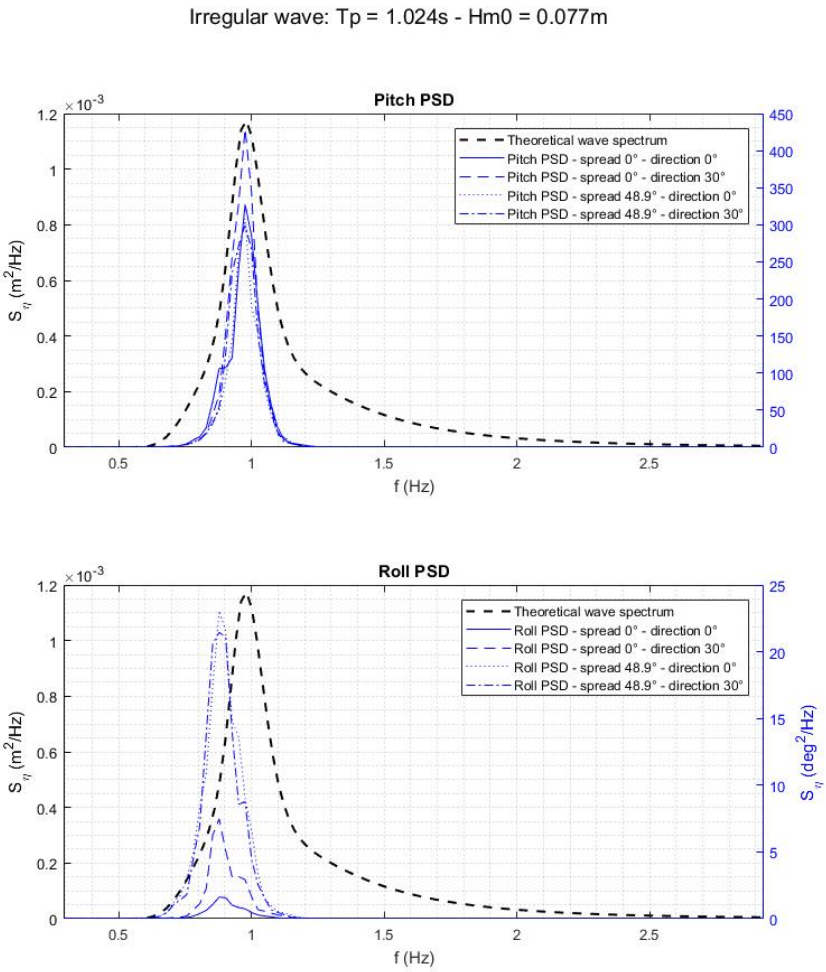

Figure 2-26 Irregular wave complex sea state analysis. Irregular wave data: Tp=1.024s and Hm0=0.077m

2.3.4 Extreme waves analysis

The analysis of the behaviour of a Wave Energy Converter in extreme waves is fundamental for a proper design of the device. In particular, in the case of ISWEC, this analysis is fundamental for correctly designing the mooring system. As indicated by the DNV rules [8] before the deployment of any structure or device at sea, it is necessary, among other things, to carry out an analysis of the reliability of the mooring system in storm conditions. As indicated by the regulations, for the analysis of mooring reliability it is necessary to carry out 10-20 tests of at least 3 hours each considering the extreme wave with a return period of 100 years. In this way you have a relevant amount of data necessary to make short-term forecasts in order to build the probability distribution over the long term. In fact, to analyse the behaviour and loads of a system moored offshore in extreme environmental conditions Extreme value theory is often employed. As indicated in several works [9-10-11], it is possible to estimate extreme values for any given time domain result variable by analysing the simulated time history of the variable using extreme value statistical methods. You may, for instance, perform a mooring analysis in an irregular sea-state and then estimate the maximum mooring line tension for a 3-hour storm. The wave considered is the following:

	Wave data			
Name	**Tp (s)**	**Hs (m)**	**gamma**	**Spread (°)**
EXT_Tp26083_Hs03192_g33_s50_dir0_Cs0_Cd0	2.608	0.319	3.3	22.7

Table 2-14 50years extreme wave data

This wave is the 50years wave of the North Sea, generated considering the JONSWAP spectrum with a spread in frequency equal to 3.3 (gamma factor) and a spread in direction equal to 50 (s factor in the cosine2s spreading function). This wave has been generated 15 times for 35 minutes with 15 different random phases between its frequency components, in order to obtain 8.75 hours of tests (almost 45 hours in in full scale).

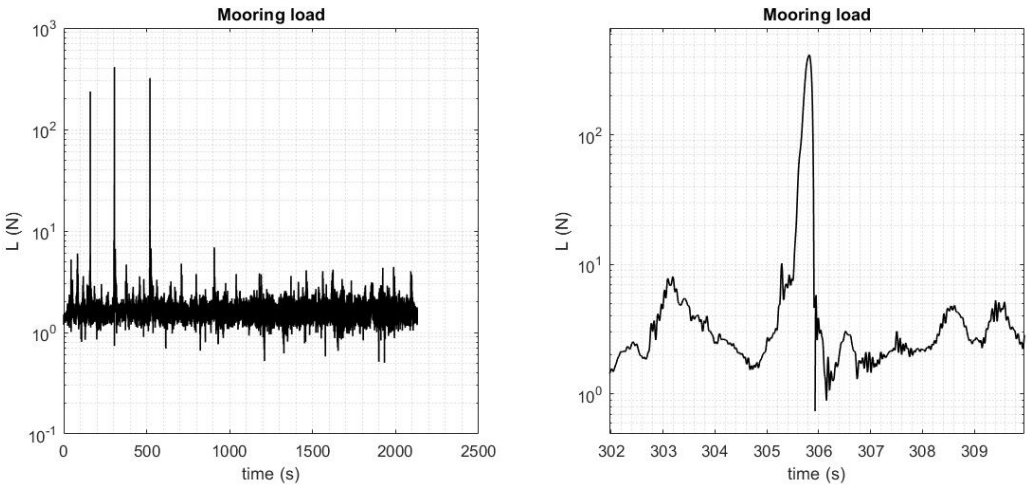

Figure 2-27 Mooring load time history

As shown by Figure 2-27, the load acting on the central joint of the mooring oscillates around its mean value, value equal to the static recall of the mooring line, composed of 3 chain sections to which are connected a jumper and a clump weight (as described in the chapter of the experimental setup). The load oscillations are due to high and low frequency dynamic components, which we will call LWF (Load Wave Frequency) and LLF (Load Low Frequency) respectively. In addition to this type of load we can also observe peaks that exceed by one or two orders of magnitude the average value of the loads (figure on the right). These events are considered extreme and, as it can be seen, they occur randomly during the storm event and are not apparently correlated to each other and to the extreme wave. In fact, when the mooring is stretched completely, the load on the mooring depends on the axial rigidity of the mooring itself and, being this rigidity equal to the rigidity of the chain, the loads are very high even in the presence of small displacements in the surge direction. These events are called snaps and are considered as extreme.

In this regard, when the object of primary interest is extrapolated into the peaks of the data, it is safest to use a model that is fitted only to the peaks of the data. This is because models that are fitted to the entire dataset tend

to be driven by features in the body of the data, which may not be relevant to the tail behaviour. In this work, according to [9-10-11], the Weibull distribution has been considered to fitting the peaks over the threshold distribution.

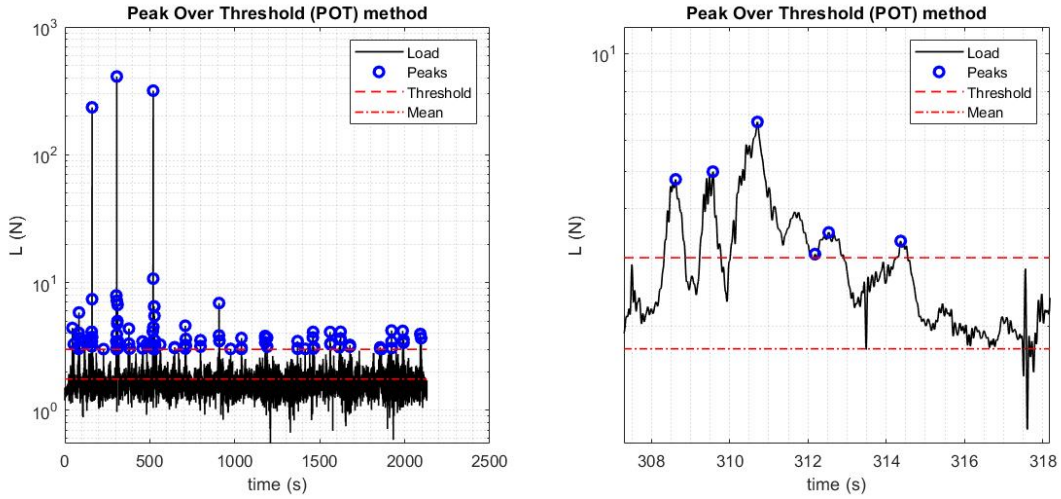

Figure 2-28 Peak Over Threshold method, identification of Load Peaks (Extreme events)

Referring to the Figure 2-28, it is possible to observe the result of the POT method: fixing an arbitrary threshold value, (in this case equal to 3 N) the maxima of each portion of load that is between a crossing of the threshold line and the next are extracted. Once the peaks have been extracted, it is necessary to check that these values are statistically independent of each other. An important assumption underpinning the maximum likelihood method, used to fit the peaks distribution in order to find the parameters of the Weibull distribution, is that the data are independent. However, this is always not the case. For example, considering all the maxima of the time history, where one low load value is likely to be followed by another. On the other hand, considering only the extreme peaks, over a threshold, successive peaks values are not dependent from the previous one.

In this regard, the complete model-fitting process is then summarised as:

- Identify the threshold which refer on to extreme events;
- Determine the values of the extreme events
- Assuming independence between these maxima, use maximum likelihood to fit the Weibull distribution

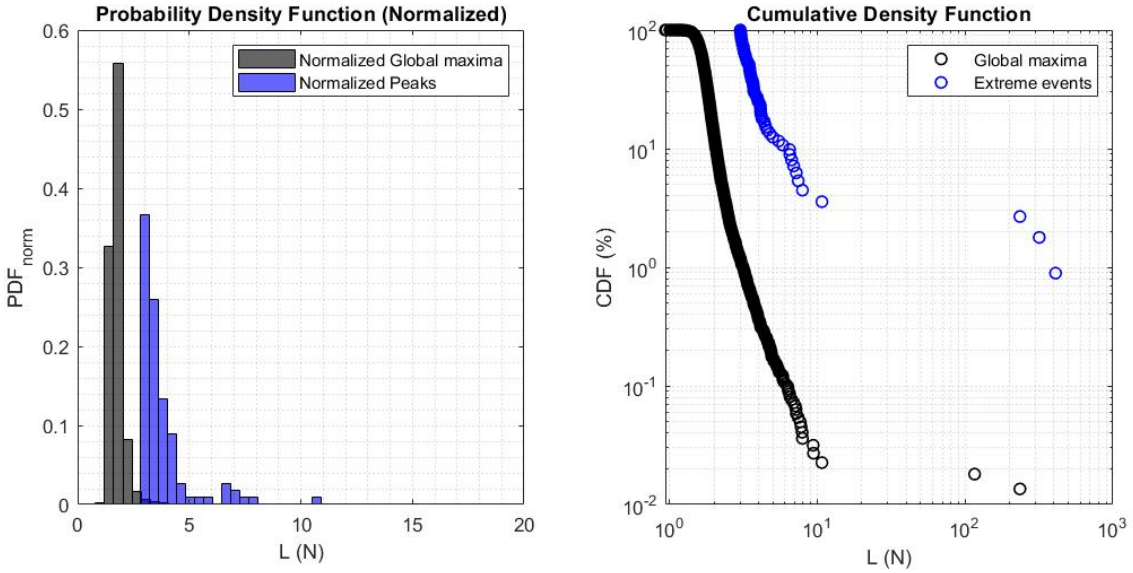

Figure 2-29 Peak Over Threshold method, effect of the threshold and amount of data considered

The Figure 2-29 shows the effect of the threshold value. The black data, refers to the probability distribution of the mooring load considering all the maxima of the load time history. Instead, the blue data refers to the extreme events only (POT method). Since the probability of extreme events is made with few points in respect to the global maxima one, the probability of the tail data of the extreme events is larger than the corresponding probability levels predicted by the global maxima distribution. The Weibull distribution fitted considering only the extreme data (POT method) will be more reliable and conservative than the one obtained considering all the peaks of the mooring load.

For the choice of the threshold value, a procedure is proposed that allows to almost completely exclude the loads characteristic of the ISWEC operating mode and to consider only the dynamic extreme loads. To do this, three different load histories were analysed, obtained by testing the device on the design wave, in the most occurring wave and energetic wave of the reference site. As shown in the Figure 2-30, first of all the mooring load has been decomposed into high-frequency components due to the wave action, which we will call TWF (Tension Wave Frequency), and low-frequency components due to the mooring system's own frequency, which we will call LF (Tension Low Frequency). Thus, one may resort to the maximum dynamic tension (T_{d-max}) encountered by a mooring system in operating condition can be approximated, as defined by DNV [70]:

$$T_{d-max} = \begin{cases} T_{WF-max} + T_{LF-sig} & for \quad T_{WF-max} > T_{LF-max} \\ T_{WF-sig} + T_{LF-max} & for \quad T_{WF-max} < T_{LF-max} \end{cases} \tag{14}$$

Where:

- $T_{WF-max} = \sigma_{T-WF}\sqrt{2\ln(N_{WF})}$ (15)
- $T_{WF-max} = \sigma_{T-LF}\sqrt{2\ln(N_{LF})}$ (16)
- $T_{WF-sig} = 2\sigma_{T-WF}$ (17)
- $T_{WF-sig} = 2\sigma_{T-LF}$ (18)

Where σ the standard deviation of the load and N the number of cycles in Low and Wave frequency of the mooring load.

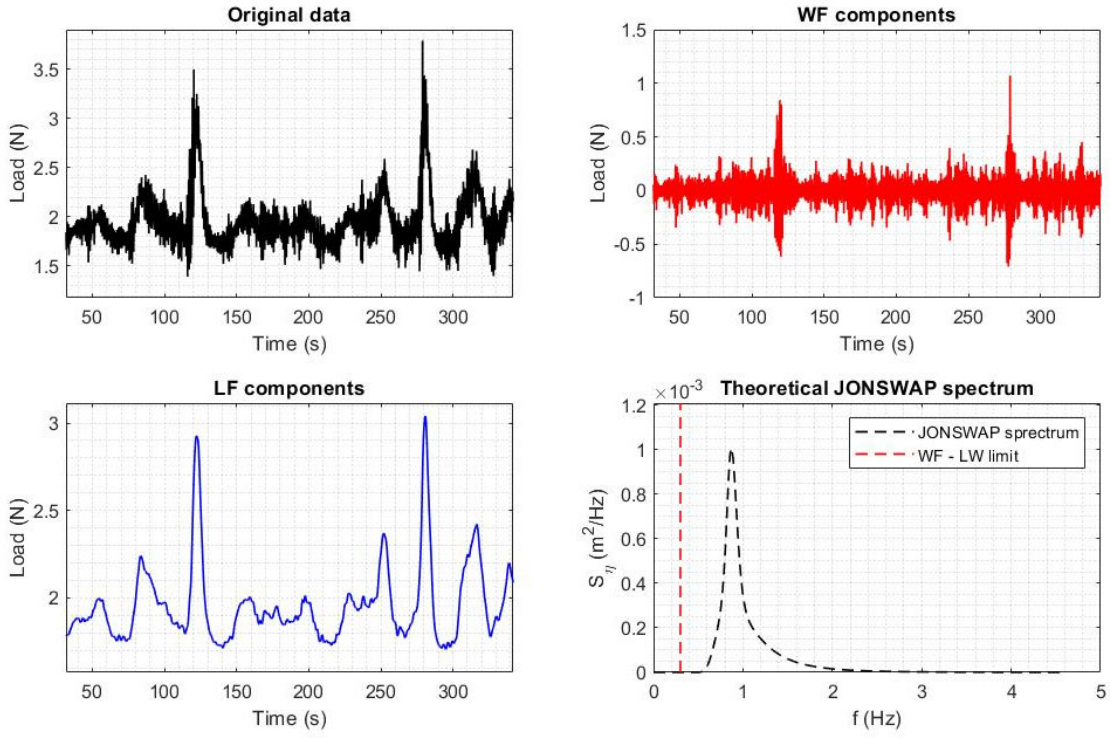

Figure 2-30 WF and LF load components in operational wave (Design Wave)

The results are shown in the Table 2-15: the maximum dynamic load in these three operating conditions is between about 2.1 and 2.6 N and, to be conservative in the calculation of the statistical distribution of extreme events 3 N is considered as threshold for extreme wave loads. It is worth to notice that the average load of the mooring in extreme wave is equal to about 1.3 N so the threshold is equal to about 2.5 times the mean load in extreme wave condition.

	Wave data				WF and LF Load results					
Name	**Tp (s)**	**Hs (m)**	**γ (°)**	**s (°)**	T mean	TWF sig	TWF max	TLF sig	TLF max	Threshold
Most Occurring	1,177	0,058	3,3	48,9	1,792	0,141	0,255	0,129	0,150	2,176
Design Wave	1,151	0,067	3,3	48,9	1,909	0,198	0,355	0,363	0,422	2,530
Most Energetic	1,373	0,096	3,3	48,9	1,886	0,221	0,395	0,308	0,356	2,589
										3

Table 2-15 Threshold identification

Once the threshold value was chosen, the POT method was applied to all 15 load stories obtained by simulating 15 times the extreme wave of the 50 years. The results are shown in Table 2-16. As can be seen, the peaks exceeding the threshold value are between 53 and 162 (100 the mean), and the mean of the extreme peak values is between 3.47 N and 12.27 N (5.34 N).

	POT results				POT results	
Name	**Tp (s)**	**Hs (m)**	**γ (°)**	**s (°)**	Number of peaks	Mean Peaks value (N)
Seed 1	2,608	0,319	3,3	22.7	97	4,50
Seed 2	2,608	0,319	3,3	22.7	112	12,27
Seed 3	2,608	0,319	3,3	22.7	83	4,23
Seed 4	2,608	0,319	3,3	22.7	109	7,58
Seed 5	2,608	0,319	3,3	22.7	76	6,00
Seed 6	2,608	0,319	3,3	22.7	73	3,73
Seed 7	2,608	0,319	3,3	22.7	78	4,38
Seed 8	2,608	0,319	3,3	22.7	53	3,47
Seed 9	2,608	0,319	3,3	22.7	136	8,28
Seed 10	2,608	0,319	3,3	22.7	162	3,60
Seed 11	2,608	0,319	3,3	22.7	126	3,57
Seed 12	2,608	0,319	3,3	22.7	117	4,94
Seed 13	2,608	0,319	3,3	22.7	101	3,92
Seed 14	2,608	0,319	3,3	22.7	101	3,61
Seed 15	2,608	0,319	3,3	22.7	109	6,16

Table 2-16 POT method results for 15 extreme waves tests

In this work peaks are fit with a three-parameter Weibull CDF:

$$F_{Load}(L) = 1 - e^{\left[-\left(\frac{L-L_{thr}}{\alpha}\right)^{\beta}\right]} \quad (14)$$

Where:

- L_{thr}: is the threshold value;
- α: scale parameter;
- β: shape parameter.

As shown in the Figure 2-31, Weibull's three-parameter distribution adapts very well to extreme events of lower intensity, bringing excellent reliability to the probabilistic distribution of these loads. On the contrary, for the highest extreme events in module (i.e. those that are beyond the threshold, equal to 16 N, indicated with the red dotted line), it is necessary to use another probability distribution because it is noted that, at the same load L, the

distribution of Weibull underestimates the prediction of the tail data. To explain this phenomenon it could be said that extreme events of low intensity are described by a different probability function than extreme events of high intensity. The study of other types of distribution (Generalized Extreme Value Distribution, Gumbel distribution) or the use of combined distributions (combined Weibull defined at times) should be referred to further works.

Fitting results					
α	β	L_{thr} (N)	T_{mean} (N)	ε_{ABS} (%)	ε_{mean} (%)
0.59	0.50	3	5.49	5.76	22.38

Table 2-17 Weibull fit results

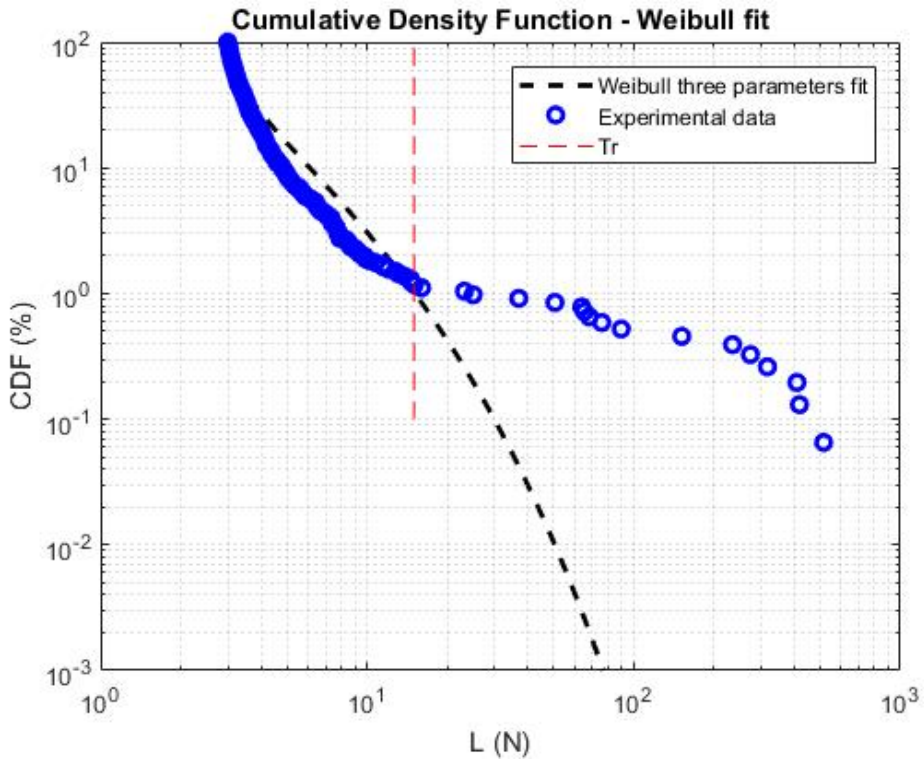

Figure 2-31 Weibull fit results

2.3.5 Pressure field analysis

As indicated in the test plan of this report, several tests have been conducted to measure the pressure field on the hull for different wave conditions. These experimental tests were conducted by sensorizing the wetted surface of the ISWEC with 11 analogue pressure sensors acquired with ARDUINO Mega 2560. These tests are not the subject of this report as the time required for an accurate assessment of the pressure fields takes longer. In any case, a line-up is reported which will be followed for the analysis of the collected data:

- Experimental evaluation of the pressure field acting on the hull in regular wave and in irregular wave
- Evaluation of the pressure range in the frequency domain and comparison of the results obtained from the numerical model of the full-scale device using the ANSYS AQWA software.
- Evaluation of the time domain pressure field in irregular wave and calculation of the forces acting on the hull surface
- Comparison with numerical model and determination of the minimum number of sensors for the calculation of the force acting on the hull in real-time.

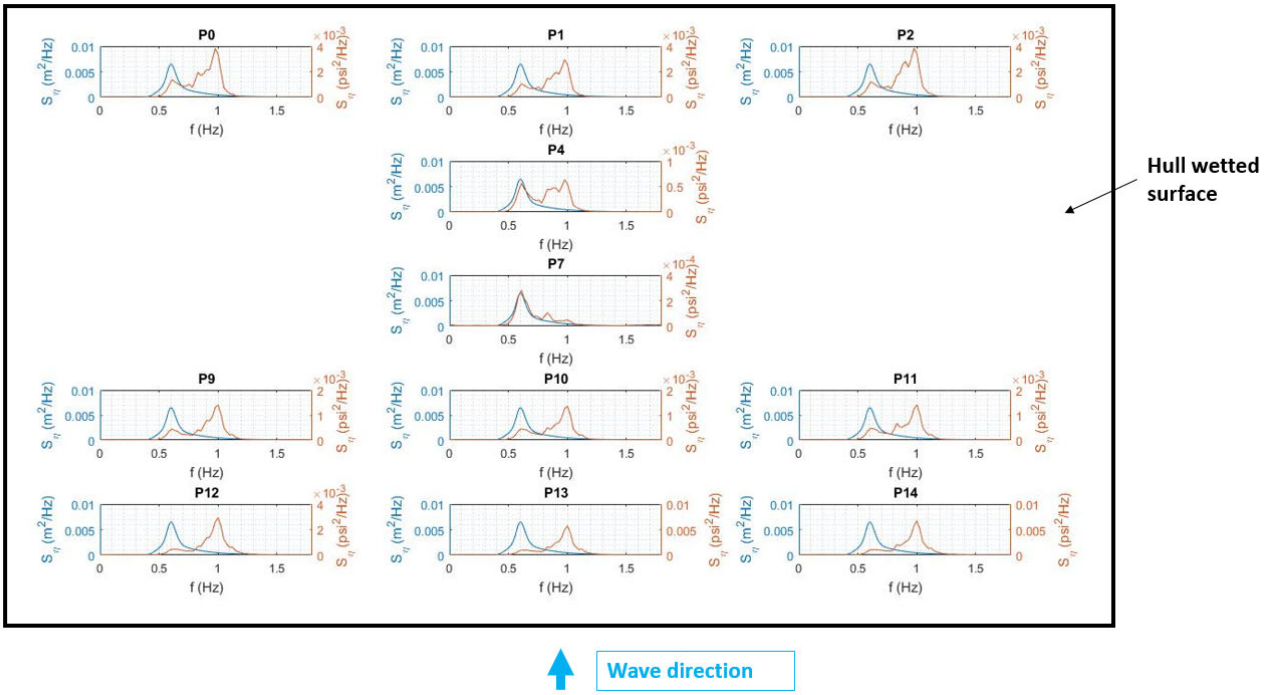

Figure 2-32 Pressure field analysis: pressure PSD in different point on the wetted surface of the hull

3 Main Learning Outcomes

3.1 Conclusions

3.1.1 Test plans and ISWEC device experimental setup

During the planning of the tests several problems that occurred during the experimental tests were not expected but overall all the fundamental tests that have been planned by the team were conducted successfully. This success of this complex experimental campaign is due principally for two reasons: a good experience of the team in the designing and building of the devices, a good planning of the tests, but most important a good communication with the wave tank facility staff. The Aalborg Wave Tank staff proved to be very helpful and interested in the project; they followed the project since the beginning and during the experimental tests their experience inside the tank and their problem-solving skills were fundamental during the tests.

An important lesson learnt during this experimental campaign is to plan easily every aspect of the tests that the team have in mind. If some aspect of the tests seems complex or hard to achieve for logistic, building, measurement problems then is better to avoid it or the get it simpler. During experimental tests the time management is very important and any operation have to be clear and as simply as possible. Flexibility is also important during experiments, every time something unexpected can go wrong and the team has to manage these episodes with calm and reorganizing the test plan.

The setup preparation for the moored device, especially for what concern the pressure sensors, was complex and challenging and presented some days of delay during the initial preparation of the tests. The calibration of the camera acquisition system was not easy as well and it caused some delays due to the complexity of the setup and the presence of unforeseen shadow points due to the wave probes setup.

3.1.2 Progress Made: For This User-Group or Technology

This experimental campaign on extreme wave and pressure field on the hull is a crucial milestone in the research progress of our team. For what concern the extreme waves, it is fundamental evaluate the behaviour of the device and mooring loads to proper design the device itself. In fact, evaluating the device only on operating condition is

not enough to have an overall evaluation of what is expected in the full-scale device once realized. Tests on single device hydrodynamics were already been carried out and the array hydrodynamics test campaign constitutes the natural following step for different interesting outcomes. Moreover, understanding the pressure field on the ISWEC hull will provide an important improvement leading to a better comprehension of the interaction between the floaters under waves and so an important improvement in forecasting the wave force both in regular and irregular wave condition. This information is fundamental for the full-scale device control law in a real sea site.

The team for the second time, thanks also for the capabilities of the wave tank, make experience of running and elaborating different type of complex waves:

- Directional waves
- Directional spectra with different spreading parameter values

This is crucial to assess the performance of the single devices in real sea state and compare the results with our wave-to-wire model in order to improve it.

Next steps are the elaboration of all the data and plan a new experimental campaign test on the full-equipped ISWEC system. In order to improve the knowledge of the wave field around the floater and its hydrodynamic behaviour and then validate the numerical model outputs, it can be interesting to test the ISWEC scaled device equipped with the gyroscope and the PTO.

3.1.3 Progress Made: For Marine Renewable Energy Industry

Extreme waves and pressure field evaluation are not so common in literature. Therefore, this experimental campaign can be a reference in this field for other works. The experimental setup has been explained in detail, starting from the scaling down procedure of the model and mooring system and describing in detail the experimental setup. Camera acquisition system, submerged load cell and analogue pressure sensor are an easy and reliable way to catch the floaters motion, both operational and extreme mooring load and pressure field on the wetted surface.

1.2 Key Lessons Learned

- Simplify the device and experimental setup reduces the failures and lead to a more reliable setup
- The correct positioning of the wave probes is fundamental in order to avoid collision with the bodies and describe the wave field around the bodies
- A good communication with the tank facility before the tests and a good collaboration during the test with the facility staff is fundamental for the success of the test campaign
- Flexibility, calm, kindness and problem solving are the most important skills during an experimental campaign
- Closing correctly the hull with glue and grey tape is enough to avoid the water to enter inside the hull
- Before and during the experiments it is fundamental to measure every single property: masses, lengths, displacements, wave probes configurations etc.
- During the test, have a test list always updated with the main properties listed, and a column with the comments of the tests
- Try to elaborate realtime the data during the test is also important in order to understand if each test was good or to repeat.
- Take a lot of pictures and videos

4 Further Information

4.1 Scientific Publications

The following publications are planned:

- Experimental evaluation of mooring loads in extreme wave condition for a floating WEC: design of the mooring system, scaling down process, experimental setup and loads evaluation in extreme sea states.
- Experimental evaluation of the pressure field on the hull of a floating WEC: experimental setup, regular and irregular wave analysis, numerical modelling and comparison with experimental results

Website:

- http://www.waveforenergy.com/
- https://www.polito.it/

5 References

[1] M. Bonfanti, "Application of a passive control technique to the ISWEC" Proceedings of the 12th European Wave and Tidal Energy Conference 27th Aug -1st Sept 2017, Cork, Ireland. (Article in a conference proceedings).

[2] S. A. Sirigu, "ISWEC design tool", International Journal of Marine Energy, Volume 15, September 2016, Pages 201-213, ISSN 2214-1669.

[3] Bracco, G., Giorcelli, E., Mattiazzo, G., Orlando, V., Raffero, M. "Hardware-In-the-Loop test rig for the ISWEC wave energy system" (2015) Mechatronics, 25, pp. 11-17. DOI: 10.1016/j.mechatronics.2014.10.007

[4] Bracco, G., Giorcelli, E., Giorgi, G., Mattiazzo, G., Passione, B., Raffero, M.,Vissio,G."Performance assessment of the full scale ISWEC system" (2015) Proceedings of the IEEE International Conference on Industrial Technology, 2015-June (June), art. no. 7125466, pp. 2499-2505. Cited 4times. DOI: 10.1109/ICIT.2015.7125466

[5] G. Bracco, E. Giorcelli, G. Mattiazzo, E. Tedeschi, and M. Molinas, 'Control Strategies for the ISWEC Wave Energy System', EWTEC 2011

[6] Bracco, G. (2012). "ISWEC: a gyroscopic wave energy converter". LAP Lambert Academic Publishing.

[7] Begovic, E. "An experimental study of hull girder loads on an intact and damaged naval ship"

[8] DNV-OS-E301 Position mooring

[9] P.J. Moriarty, W.E. Holley, and S.P. Butterfield, "Extrapolation of Extreme and Fatigue Loads Using Probabilistic Methods", Technical report, National Renewable Energy Laboratory

[10] Toft, Henrik Stensgaard; Sørensen, John Dalsgaard, "Extrapolation of Extreme Response for Wind Turbines based on Field Measurements", Safety, Reliability and Risk of Structures, Infrastructures and Engineering Systems

[11] Simon Ambühl, Martin Sterndorff, John D. Sørensen, "Extrapolation of extreme response for different mooring line systems of floating wave energy converters", International Journal of Marine Energy,Volume 7, 2014, Pages 1-19, ISSN 2214-1669

[12] Hsu, Weiting. (2017). Dynamic Modeling and Extreme Tension Analysis of Mooring System for a Floating Offshore Wind Turbine.

[13] DNV. Design of Floating Wind Turbine Structures. DNV-OS-J103. Hovik, Norway: Det Norske Veritas; 2013.